Supramolecular Polymers in Inhomogeneous Systems

Promotor:	prof. dr. G. J. Fleer, persoonlijk hoogleraar bij de leerstoelgroep Fysische Chemie en Kolloïdkunde
Copromotor:	dr. ir. N. A. M. Besseling, universitair docent bij de leerstoelgroep Fysische Chemie en Kolloïdkunde

Samenstelling promotiecommissie:

dr. M. Dijkstra	Universiteit Utrecht
prof. dr. D. Frenkel	AMOLF, Amsterdam
dr. ir. P. P. A. M. van der Schoot	Technische Universiteit Eindhoven
prof. dr. H. van Amerongen	Wageningen Universiteit

Supramolecular Polymers in Inhomogeneous Systems

H. J. A. Zweistra

Proefschrift

ter verkrijging van de graad van doctor

op gezag van de rector magnificus

van Wageningen Universiteit,

prof. dr. M. J. Kropff,

in het openbaar te verdedigen

op woensdag 3 januari 2007

des namiddags te half twee in de Aula.

ISBN 90-8504-552-5

Contents

Chapter 1

General Introduction

1.1. Polymers

Life is full of polymers. Any book on molecular biology (e.g. Ref.[1]) will show how much life on earth depends on polymers. To begin with, organisms use polymers of different types for structural purposes (cellulose), storage of energy (starch, glycogen), and information (DNA), not to mention the countless vital tasks that are performed on a cellular level by polymers like proteins and RNA. Realizing how much we need polymers for sustenance makes it indeed seem hard to conceive that extraterrestrial lifeforms can survive *without* polymers. In addition to their biological importance, polymeric substances play an important role in our daily lives as well. Materials like rubber, plastic, all natural fabrics, paper, and food additives like corn starch and gelatin consist entirely or to a large extent of polymers. Less visible perhaps but equally important industrially: polymers can act as surface-modifying agents. They are used to control colloidal stabilization,[2] prevent the adhesion of biological material,[3] and so on.

Not surprisingly, polymers are objects of major technological and scientific interest. The sheer abundance of polymeric species used in industry merits technological interest, while scientists are intrigued by the common principles that define all polymeric compounds.

The common feature of the diverse class of polymeric molecules is the shape: long and thin. Polymeric substances consist of many individual subunits (called *monomers*) that are linked together to form a threadlike structure. If the monomers are linked by

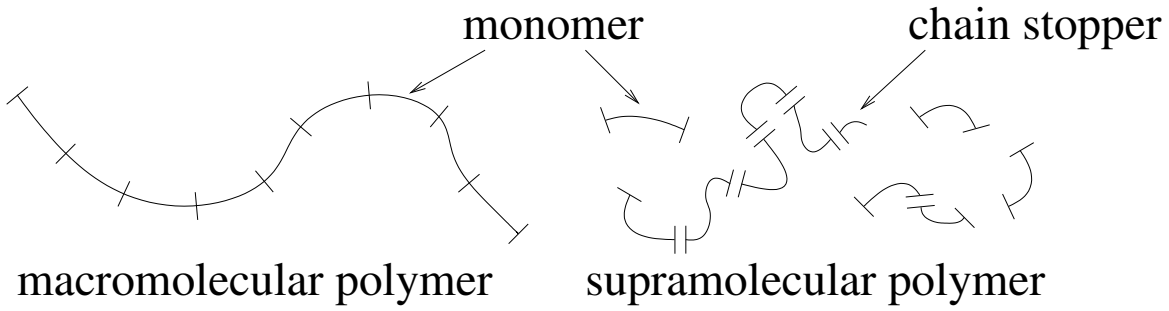

Figure 1.1. Comparison of macromolecular polymers and supramolecular polymers. The macromolecular polymer consists of monomers that are joined covalently, while the monomers of supramolecular polymers are connected by reversible bonds. A chain stopper is also indicated.

covalent bonds, then the entire polymer is a single molecule which is called a *macromolecule* (see Fig. 1.1). In many cases the nature of the monomers is unimportant. For example, the unique rheological behavior of polymers is almost entirely a function of chain length, not of the shape of the monomers.[4] Chain length is therefore the most prominent property that defines polymeric behavior.

1.2. Supramolecular polymers

The chain lengths of macromolecular polymers cannot generally be altered once the polymers have been synthesized. Some time ago, scientists started to develop polymers with reversible bonds between the monomers. Such polymers are known as *reversible supramolecular polymers* or simply *supramolecular polymers* because the polymeric chain consists of separate molecules that form a supramolecular structure (Fig. 1.1). These compounds have many features in common with ordinary polymers, but the reversible nature of the bonds introduces behavior that is not found in systems containing ordinary polymers. For example: supramolecular assemblies can switch between linear chains and rings, provided that the backbone of the chain is flexible enough to fold back onto itself.

Many types of monomers of supramolecular polymers have already been synthesized.[5] They typically consist of two linking groups that are connected by a spacer (see Fig. 1.1). It was found that many types of physical interactions are suitable to reversibly link the monomers. This has led to a large variation in the nature of the reversible bond that connects the monomers. For example, there exist linking groups based on specially designed multiple hydrogen-bonding groups,[6] metal-ligand interactions,[7] and oligonucleotides.[8]

These monomers should fulfill an important criterion: they should have exactly two linking groups to form linear chains or rings. Monomers with only one linking group are known as 'chain stoppers', since the supramolecular chain is terminated if such a monomer is incorporated (Fig. 1.1). It turns out that small amounts of chain stoppers are very destructive to the chain-forming capabilities of supramolecular polymers.[9, 10] Unfortunately, they frequently occur as an unwanted byproduct of the synthesis of monomers and they are very difficult to remove by conventional methods.[5, 9, 11] In chapter 5, we propose a new method to remove chain stoppers from supramolecular polymer solutions. The chain stoppers can be removed by inducing phase separation.

Supramolecular polymer systems usually contain chains of varying length. These systems can therefore be characterized by the average number of segments per chain, which is denoted by $\langle N \rangle$. Experiments have shown that $\langle N \rangle$ is sensitive to variations in temperature, concentration, nematic ordering of the environment and shear.[12] Very often, there is a complex coupling between these effects. For example, applying shear

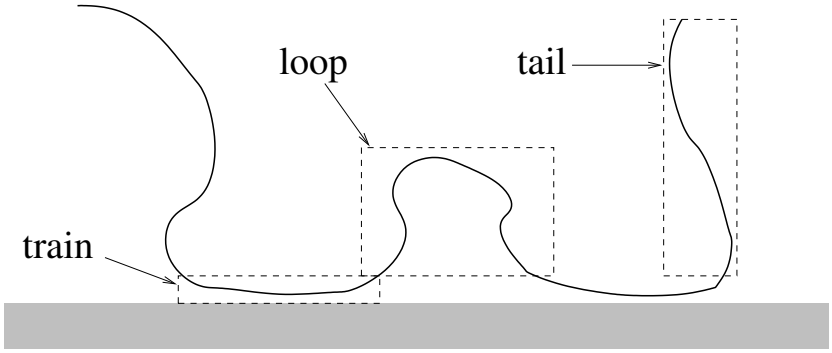

Figure 1.2. Schematic representation of an adsorbed polymer molecule. The surface is indicated in grey.

may lead to rupture of the chains, but at the same time align the chains, which enhances chain formation. It therefore comes as no surprise that supramolecular polymer systems exhibit complex rheological behavior. It is generally thought that usage of supramolecular polymers in industrial processes will increase in the near future.[13] If we obtain a better understanding of these systems, we can tune their properties to fit the requirements of the industrial process.

This thesis does not deal with the rheology of supramolecular polymers but focuses on the equilibrium behavior. Since polymers are often used to alter the properties of surfaces, there is also a considerable interest in supramolecular polymers at interfaces. Chapters 2 and 3 focus on the properties of adsorbed supramolecular polymers. We refer to an *adsorbed chain* if at least one of the segments of the chain is next to the interface. Unless the segments have a special affinity for the surface, the polymers tend to avoid the surface for entropic reasons.[14] When the adsorption energy per segment is larger than a certain threshold value, the chains will adsorb at the surface. The shape of a flexible polymer usually alters when it is adsorbed from solution. In chapter 2, it is shown that the structural change upon adsorption has an important effect on $\langle N \rangle$.

A schematic representation of an adsorbed polymer molecule is depicted in Fig. 1.2. Three substructures of the adsorbed chain are recognized: trains, loops and tails. In the context of polymer adsorption, a train is a sequence of segments that are next to the surface. A loop is a part of a chain that is in solution but is connected to trains at the ends. Finally, the tails are the 'loose ends' of the adsorbed chain. Let us denote the number of trains, loops and tails of an adsorbed supramolecular assembly as n_{tr}, n_{lp}, and n_{tl}, respectively. In the case of a linear chain, $n_{tr} = n_{lp} + 1$ and $0 \leq n_{tl} \leq 2$. If the assembly is a ring, n_{tl} is obviously equal to 0. Unless the ring is entirely adsorbed as a chain, $n_{tr} = n_{lp}$.

The average number of segments that reside in trains, relative to the total number of segments of the adsorbed chains, is indicated by ν_{tr}. The parameter ν_{tr} depends on experimental conditions. The surface with a single adsorbed molecule with pronounced

loops and tails as depicted in Fig. 1.2 is the situation of dilute solution and weak adsorption. When the adsorption energy per segment is sufficiently high, then adsorbed polymers will completely adsorb as trains at low concentrations.[14] A systematic study of supramolecular polymers in the strong adsorption regime ($\nu_{tr} \approx 1$) is presented in chapter 3 of this thesis.

In this thesis, we consider supramolecular polymers in phase-separated systems and in systems which contain interfaces. Both types of systems are known as *inhomogeneous systems*. Therefore both the title and the main focus of this thesis are: "Supramolecular polymers in inhomogeneous systems".

1.3. Simulations

1.3.1. Why simulations?

Contemporary research in physical chemistry is very often an interaction between experimental evidence, analytical theories and simulations. Simulations do not yield 'real' proof like experiments do. Nor are the results of simulations as generally applicable as an analytical expression that describes a certain phenomenon. So why would one use simulations to elucidate the mechanisms of the molecular world?

It turns out that some theories yield problems that are very hard to solve unless severe approximations are used. Furthermore, simulations can yield information that is impossible or extremely difficult to obtain by means of experiments. Often simulations yield new insights. As a result, simulations play an important role in physical chemistry, but they should be used in conjunction with a theoretical framework and experimental validation.

1.3.2. Choice of model system

Supramolecular polymers are a diverse group of molecules which have many features in common. The aim of the present study is to describe generic properties that are found among all types of supramolecular polymers. It is in principle possible to mimic in great detail the specific interactions of a supramolecular compound that one intends to study. Realism is then the special aim of the simulation, and the level of detail should be as high as computationally possible. The approach in this thesis is nearly the reverse: the model should have the *least* amount of complexity while retaining the essential features of supramolecular polymers. This approach has several benefits. Since the model is kept very simple,

- the observed properties are not limited to a specific system;
- the results are more easily understood because of the small number of model parameters;
- the computational demands of the simulation are reduced.

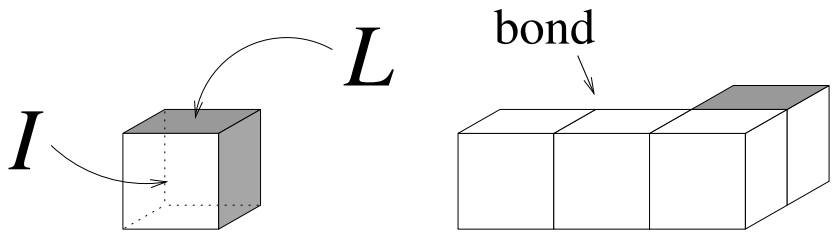

Figure 1.3. The model for supramolecular polymers that was used in this thesis. Two types of faces are found on the monomers: linking faces and indifferent faces, which are denoted L and I, respectively. A bond is formed if two linking faces of two adjacent monomers point towards each other.

Since the results are so general, they do not reproduce experimental data quantitatively. What can be obtained from these simulations are insights in the trends, not precise numbers.

We used an extremely coarse-grained model of supramolecular polymers. The model was constructed as follows. A good start is to divide space into lattice sites with coordination number q. Both monomer and solvent molecules occupy one lattice site. We can assign an energy to a contact between molecules of two different types. This model is known as the 'Ising model'.[15] If the contact energy between the monomers is sufficiently positive, 2- or 3-dimensional systems will separate into two phases. Calculating the compositions of the coexisting phases is a classic problem in statistical physics. One particularly efficient method to solve this problem (and more complex problems) is presented in chapter 4.

The monomers of the supramolecular chain should possess a certain affinity for each other in order to form chains. However, affinity is necessary but not sufficient: when the monomers are simply isotropic, then amorphous 'blobs' will be formed, not linear chains. To solve this problem, we must add directionality to the model: the concept of *faces*. A face is a type of side on the molecule. We distinguish between different kinds of faces, and a certain energy is assigned when two faces of adjacent molecules are in contact with each other. Each molecule is engaged in q interactions with its neighbors.

For monomers we will distinguish two types of faces: 'linking faces' and 'indifferent faces'. If two monomers in adjacent lattice sites have a linking face pointing towards each other, a bond is formed between these monomers (Fig. 1.3). Therefore each molecule should have exactly two linking faces to form linear structures. They may be on opposite sides of the monomer, or make a 90° angle. If the linking faces are perpendicular with respect to each other, the molecule is 'bent'. Incorporating a bent molecule in the supramolecular chain results in a bend of the chain at that position (Fig. 1.3). We can adjust the stiffness of the supramolecular chain by assigning a positive energy to each bent molecule. Chain stoppers are also very easily modeled: these are molecules with $q - 1$ indifferent face and 1 linking face.

1.3.3. Finding the distributions of monomers

There are several ways of assigning faces to different directions on a molecule. These may be called molecular *states*. For example, monomers have $\binom{q}{2}$ states*, chain stoppers have $\binom{q}{1} = q$ states while isotropic molecules have only one state. We can place the molecule models inside a simulation box in order to study the properties of the system. It is obvious that there are many, many different ways to put the monomers in the simulation box, unless the box is extremely small. A possible realization of the simulation box is named a configuration. If the total number of states of all molecules present is equal to $\mathcal{N}$, then each configuration represents a single point in the $3\mathcal{N}$-dimensional configuration space, since there are 3 spatial coordinates for each state.

The free energies of the configurations vary widely. In an isothermal system, the low-energy configurations are the most probable configurations to encounter in reality. A measurable quantity corresponds to a weighted average over the entire configuration space. The weighted average of the occupation of lattice sites over the entire configuration space is called the distribution of monomers over the system. Finding the monomer distribution is important as it yields structural and thermodynamic information about the system.

It is in principle possible to generate every possible configuration, determine the energy of each configuration and perform a weighted sum over all configurations to find the exact averages of the model system under study. This approach is used in exact enumeration studies.[14] However the number of configurations increases very rapidly with the size of the system, the number of molecules and the number of states. On present-day computers, the time needed to generate all possible configurations may easily exceed the age of the universe. Solving this problem is and has been a major and fundamental challenge in statistical mechanics. Over the years, several methodologies have been developed that tackle this problem in different ways. The methods that were used to obtain the results described in this thesis are:

Metropolis importance-sampling simulations: This method is more commonly known as a Monte Carlo simulation. Instead of generating all configurations, this method replaces integration over the entire configuration space by a walk through configuration space. A simulation is therefore a succession of steps through configuration space. The formalism itself does not impose any restrictions to the way the steps are generated, but it does impose that the probability of performing the next step depends on U_{step}, the energy difference between the configuration before and after performing the step. The usual choice for this probability is:

- 1 if $U_{step} \leq 0$;

*The binomial coefficient $\binom{n}{m} \equiv \frac{n!}{(n-m)!m!}$ is the number of ways of picking m unordered outcomes from n possibilities.

- $\exp(-U_{step}/kT)$ if $U_{step} > 0$.

where k is Boltzmann's constant and T the temperature. The average of this random walk is then equal to the average of the entire configuration space for a sufficiently long walk.

Mean-field calculations: The distribution of monomers is determined by the potentials that each monomer individually experiences. The distribution functions can be calculated directly if the potentials are approximated. A common approach is to calculate the potentials based on the local concentrations of molecules. This is equivalent to the Flory level of approximation. As a first order correction, we can include the occurrence of pairs of sites. This level of approximation is called *quasi-chemical*, because it mimics the local structure of the molecules much better than the Flory approximation. Long-range correlations are then ignored but the directionality of the monomers is taken into account which is important because of the directional nature of the supramolecular bond. Analytical expressions are available for isotropic, homogeneous systems. For inhomogeneous systems, no such analytical expressions exist and the distribution must then be found numerically by means of a self-consistent field calculation. This is the case for both levels of approximation.

There is of course at lot more to be said about these methods, but this is beyond the scope of this introduction. A thorough treatment of the fundamentals and applications of Monte Carlo simulations can be found in Ref.[16] For more information about the application of the mean-field calculations to homogeneous and inhomogeneous systems containing supramolecular polymers, see Ref.[17]

1.4. Outline of this thesis

This thesis consists of two parts of two chapters each. The first part (chapters 2 and 3) is directed toward the adsorption of supramolecular polymers at an interface. These chapters describe numerical results obtained by means of the quasi-chemical method as described in section 1.3. In chapter 2, effects of adsorption on the mean chain length of supramolecular polymers is investigated. The adsorbed amount of supramolecular polymers is the focus of chapter 3. We describe the change of the adsorption isotherms upon varying the model parameters. From this, information can be obtained about the adsorption and desorption properties of supramolecular and macromolecular polymers.

The second part of this thesis (chapters 4 and 5) focuses on phase separated systems. These results were obtained by means of Monte Carlo simulations. Chapter 5 proposes a new method to remove chain stoppers by means of inducing phase separation, whereby the relative concentration of chain stoppers is different in the two phases. However, calculating the compositions of coexisting liquid phases modeled on a lattice is a non-trivial task. Therefore, we developed a new technique to deal with this problem

effectively: the Helmholtz ensemble. The methodology of this technique is described in chapter 4. The Helmholtz-ensemble method proves to be very accurate and efficient in calculating phase coexistence of lattice fluids. It was therefore applied to supramolecular polymers (chapter 5) in order to estimate the effectivity of the proposed purification method.

References

[1] J. M. Berg, J. L. Tymoczko, L. Stryer, and N. D. Clarke, *Biochemistry*, Freeman, New York, 5th edition, 2002.

[2] D. H. Napper, *Polymeric Stabilization of Colloidal Dispersions*, Academic Press, London, 1983.

[3] E. Currie, W. Norde, and M. A. Cohen Stuart, Adv. Coll. Int. Sci. **100-102**, 205 (2003).

[4] M. Doi and S. F. Edwards, *The Theory of Polymer Dynamics*, Clarendon Press, Oxford, 1986.

[5] L. Brunsveld, B. J. B. Folmer, E. W. Meijer, and R. P. Sijbesma, Chem. Rev. **101**, 4071 (2001).

[6] P. S. Corbin and S. C. Zimmerman, *Hydrogen-Bonded Supramolecular Polymers*, chapter 4, Supramolecular polymers (Ed. A. Ciferri), Marcel Dekker, New York, 2000.

[7] T. Vermonden et al., Macromolecules **36**, 7035 (2003).

[8] E. A. Fogleman, W. C. Yount, Y. Xu, and S. L. Craig, Angew. Chem. Int. Ed. **41**, 4026 (2002).

[9] R. Sijbesma et al., Science **278**, 1601 (1997).

[10] W. Knoben, N. A. M. Besseling, L. Bouteiller, and M. A. Cohen Stuart, Phys. Chem. Chem. Phys. **7**, 2390 (2005).

[11] G. Armstrong and M. Buggy, J. Mat. Sci. **40**, 547 (2005).

[12] M. E. Cates and S. J. Candau, J. Phys.: Condens. Matter **2**, 6869 (1990).

[13] A. Ciferri, *Supramolecular Polymers*, Marcel Dekker, New York, 2000.

[14] G. J. Fleer, M. A. Cohen Stuart, J. M. H. M. Scheutjens, T. Cosgrove, and B. Vincent, *Polymers at Interfaces*, Chapman and Hall, London, 1993.

[15] T. L. Hill, *An Introduction to Statistical Thermodynamics*, Addison-Wesley, London, 1960.

[16] D. Frenkel and B. Smit, *Understanding Molecular Simulation*, Academic Press, London, 2002.

[17] J. van der Gucht and N. A. M. Besseling, Phys. Rev. E **65**, 051801 (2002).

Chapter 2

Mean Chain Length of Adsorbed Supramolecular Polymers*

Abstract

We present a theoretical study of reversible supramolecular polymers near an adsorbing surface. Mean chain lengths for free and adsorbed supramolecular polymers were calculated for a broad range of concentrations. As far as we know, this is the first report that describes a regime where the mean chain length *decreases* with increasing monomer concentration. It is shown that this anomalous behavior is caused by a change of the structure of the adsorbed layer.

Polymers with reversible bonds have provoked a lot of excitement in the scientific community in recent years. Many new types of these novel polymers have been synthesized recently, and these compounds have become known in the field as *supramolecular polymers*.[1] It is to be expected that materials with tailored mechanical and structural properties can be devised from these polymers, since the chain length of supramolecular polymer can be changed reversibly.[1] This gives supramolecular polymers distinct advantages over ordinary polymers with a quenched weight distribution. For example, supramolecular polymers can be used to regulate colloidal stability in suspensions or modify the properties of a surface in ways that are qualitatively different from ordinary polymers.[2] To obtain an understanding of the behavior of supramolecular polymers is crucial in controlling the properties of supramolecular materials.

We present a theoretical study of supramolecular polymers in this Letter. The arguments proposed here are kept general, so the results presented in this chapter are applicable to any material containing linear reversible aggregates. Examples of such systems are liquid sulphur,[3] selenium,[4] actin filaments,[5] and wormlike micelles.[6, 7] Moreover, the results presented here are also valid for ordinary polymers with the same size distribution (e.g. condensation polymers).[8]

Supramolecular polymers consist of monomers that are joined by reversible bonds. The number averaged degree of polymerization $\langle N \rangle$ of supramolecular polymers is the most interesting parameter to characterize the system because it depends on the system in the case of supramolecular polymers, but is constant for ordinary polymers. In this Letter, a comparison is made between the average chain length of free chains in solution, $\langle N_{bulk} \rangle$, and the average length of chains that are adsorbed to a surface, $\langle N_{ads} \rangle$.

*Published as: H. J. A. Zweistra and N. A. M. Besseling, Phys. Rev. Lett. **96(7)**, 078301, (2006).

While expressions are available for $\langle N_{bulk} \rangle$, the calculation of $\langle N_{ads} \rangle$ has not yet been addressed in literature. This issue is essential in understanding the behavior of supramolecular polymers near interfaces. Here, we report numerical calculations of $\langle N_{ads} \rangle$ and show that $\langle N_{ads} \rangle$ has a qualitatively different concentration dependence than $\langle N_{bulk} \rangle$.

Predictions for the weight distribution of supramolecular chains in a homogeneous, isotropic environment go back to a classic paper by Flory.[9] The Flory theory was derived in the context of reacting condensation polymers, but the theory is also applicable to supramolecular polymers. Within the Flory mean-field approximation, it is assumed that the scission energy E_{scis} is independent of chain length and that long chains are formed. It can then be shown[6] that

$$\langle N \rangle \approx \sqrt{\phi} \exp\left(\frac{E_{scis}}{2kT}\right). \tag{2.1}$$

Here ϕ is the volume fraction of monomers, k is Boltzmann's constant and T is the temperature. The result (2.1) does not depend on the stiffness of the chain.

Lattice models can be useful if a thorough analysis of the model system is desirable. We will consider a system that is partitioned into cubic lattice sites with lattice spacing unity. Each lattice site has q neighboring sites, where q depends on the dimensionality of the system. The sites are occupied by either a solvent molecule or a monomer. The solvent molecules are engaged in isotropic interactions with their neighbors. On the other hand, monomers have different faces, and the interaction with a neighboring site therefore depends on their mutual orientation. The monomers have two linking faces, denoted by L, which have a special affinity for each other. The other $q-2$ 'indifferent' faces on the monomer are designated by the letter I. A bond is then formed if linking faces of two adjacent monomers are directed toward each other, and a chain consists of monomers which are connected by such bonds.

An energy u_{ij} is assigned to each contact between a face of type i and a face of type j. For instance, the energy of a contact between two linking faces, u_{LL}, has to be negative in order to obtain appreciable chain formation. Obviously, u_{LL} is related to E_{scis} if all other interactions are zero: $u_{LL} = -E_{scis}$.

The stiffness of the chain is controlled by means of the energy u_{bent}, which is assigned to each monomer of which the two linking faces are perpendicular to each other. u_{bent} can be related to the persistence length ℓ_p: $\ell_p = 1 + \frac{1}{4}\exp(u_{bent}/kT)$ in a cubic lattice.[10]

Van der Gucht and Besseling recently applied the Bethe-Guggenheim, or quasi-chemical, approach to supramolecular polymers in homogeneous and inhomogeneous systems.[2, 11, 12] Correlations in the occupation of adjacent lattice sites are accounted for in this approach, but pairs of sites are considered to be occupied independently. The Bethe-Guggenheim approach can therefore be regarded as a first-order correction over

the random-mixing approximation, in which the occupation of lattice sites is assumed to be stochastically independent.

Usually, only numerical results can be obtained at the level of the Bethe-Guggenheim approximation, but in some limiting cases, analytical results can be found. Van der Gucht and Besseling derived an expression of $\langle N \rangle$ for free chains in a homogeneous, isotropic environment.[11] Their result is

$$\langle N \rangle = 1 + \sqrt{\frac{\phi}{q/2 - \phi}} \exp\left(\frac{-u_{LL}}{2kT}\right). \tag{2.2}$$

The above equation gives a more accurate expression of $\langle N \rangle$ than Eq. (2.1). It is exact within the Bethe-Guggenheim approximation. Note that the above equation collapses to Eq. (2.1) in the limit of long, linear chains and low monomer concentrations.

Moreover, Eq. (2.2) allows us to compare the mean chain lengths for different dimensionalities. For example, in the three-dimensional simple cubic lattice used here, $q = 6$, and $q = 4$ in the corresponding two-dimensional square lattice. In the concentrated regime, assuming that long chains are formed, we find that $\langle N \rangle_{cubic} : \langle N \rangle_{square} \approx 1 : \sqrt{2}$. In general, a lower dimensionality of the system leads to a higher average chain length.

To sum up, both the Flory and the more accurate Bethe-Guggenheim approach predict that $\langle N \rangle$ of free chains increases monotonically with concentration. This result will be compared with the mean chain lengths of adsorbed chains.

Direct Monte Carlo methods are unsuitable to calculate $\langle N_{ads} \rangle$ for realistic chain lengths, because E_{scis} is easily of order $10kT$.[1] Therefore, the acceptance probability of breaking a chain will be very low, and hence excessive equilibration times will be needed. Therefore $\langle N_{ads} \rangle$ will be calculated by means of the Bethe-Guggenheim approach, because this leads to a far better description of polymeric behavior than random-mixing mean-field theories can provide. It was shown by Dickman and Hall[13] that the Bethe-Guggenheim approach gives a much better description of the equation of state than the Flory method. Unfortunately, no analytical expressions are available in this case, so $\langle N_{ads} \rangle$ has to be calculated numerically.

Still, indirect correlations between monomers are approximated, and the occurrence of rings is disregarded. Although the severity of the approximations is not exactly known, it is obvious that the description becomes better at high monomer densities, since the local environment of the monomers is then well captured by a mean-field approach. Furthermore, the calculations are more accurate when long chains are formed, because the probability of ring closure then becomes extremely low. Both these conditions are met near the interface for a large concentration range (nearly full coverage, $\langle N \rangle \gg 1$). It is therefore not to be expected that a more elaborate type of calculation will lead to different conclusions than ours.

It should be noted that a nematic environment promotes chain formation.[14] While this effect is ignored in the random-mixing approximation, it is included to some extent

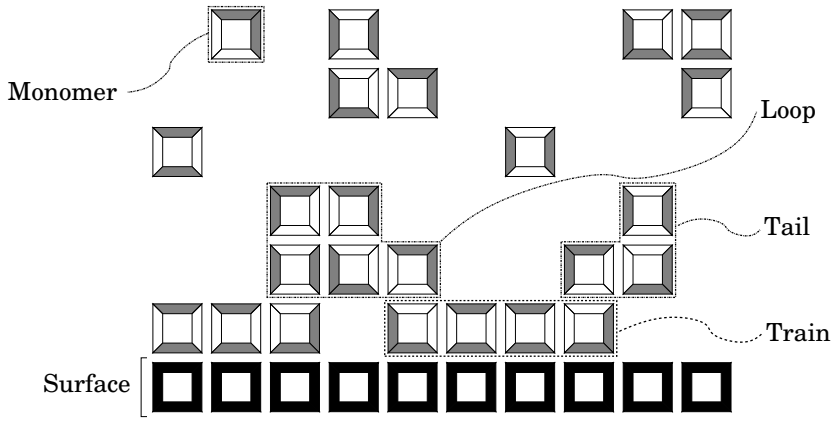

FIGURE 2.1. Two-dimensional representation of the lattice model described in this chapter. Monomers are indicated by the squares with two white sides and two grey sides, which indicate the linking and indifferent faces respectively. The surface is represented by black squares. Solvent molecules are not depicted. A loop, a tail and a train are also indicated.

in the present approximation. However, it remains questionable whether lattice models are suitable to study condensation of rods on the surface.[15] The results for flexible chains might therefore be more accurate than the results for very stiff polymers.

The lattice model described above is therefore extended to account for the presence of an interface. Our system of interest is then a wide slit with a reflecting boundary parallel to the surface. The slit is in equilibrium with a large, homogeneous reservoir with monomer concentration ϕ. It has been checked that the slit width is large enough that adsorption can be assumed to occur on an isolated surface.

The surface is also covered with faces of a certain kind, they are hereafter referred to as S. Adsorption of the supramolecular polymers is governed by the interaction between the faces on the surface and those on the monomers. The case of adsorbed chains that are in full equilibrium with the chains in the bulk, is of interest here. A schematic representation of the model system is shown in Fig. 2.1.

The mean chain length and other properties of the system can be calculated numerically if the distribution of monomers over the system is known.[11] This distribution depends on ϕ, T, u_{bent}, and the contact energies $\{u_{ij}\}$. The appropriate partition functions and minimization scheme are described elsewhere.[11, 16]

A chain is defined to be 'adsorbed' if at least one monomer of the chain is adjacent to the surface. Using this definition, the average length of the adsorbed chains can be calculated from the occupation of lattice sites in the same way as mean lengths of ordinary chains in a homogeneous environment are calculated.[11] Similarly, the mean length of substructures of adsorbed chains can be calculated. A train is defined as a sequence of monomers in the lattice layer adjoining the surface, a loop connects two trains, and a tail is connected at one end to a train (Fig. 2.1).

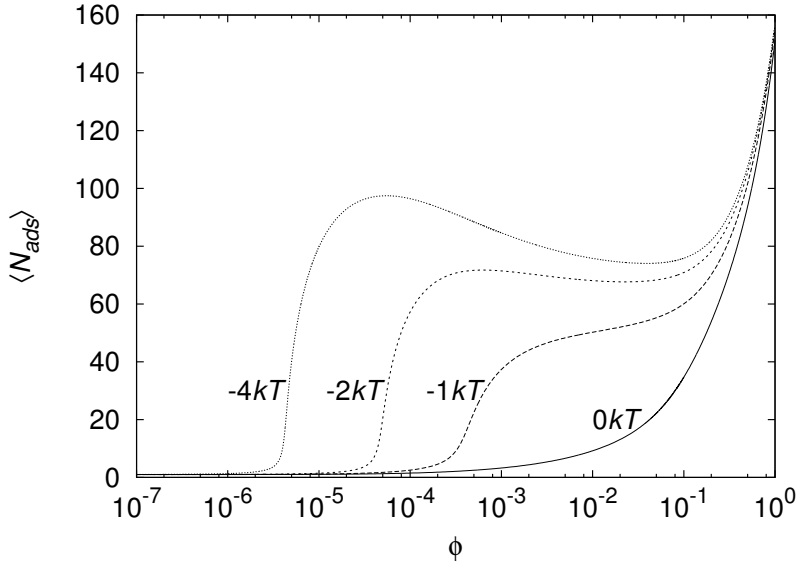

Figure 2.2. The mean chain length of the adsorbed chains versus the monomer concentration in the reservoir. Results for monomers with different adsorption energies u_{IS} (in units kT) are shown. Parameters: $u_{LL} = -10kT$, $u_{bent} = 0kT$.

The mean length of the adsorbed chains is plotted in Fig. 2.2 against bulk monomer concentration for different adsorption energies. Note the emergence of a peculiar non-monotonic concentration dependence of the chain length for $u_{IS} \lesssim -2kT$. This behavior is qualitatively different from Eqs. (2.1) and (2.2) since both formulae predict that $\langle N \rangle$ increases with ϕ at all concentrations. The plots in Fig. 2.2 merge at $\phi \to 1$ because adsorption energy is irrelevant in a polymer melt: a monomer is then replaced by another monomer upon removal from the surface.

Mean chain lengths of adsorbed supramolecular polymers with varying flexibility are shown in Fig. 2.3. Figure 2.3(a) shows that the non-monotonic concentration dependence is not found for very stiff polymers. This is related to the fact that stiff chains do not form loops and tails, but instead remain adsorbed as trains over the entire concentration regime. Figure 2.3(b) shows that, at low ϕ, even flexible monomers adsorb predominantly as trains, and loops and tails are formed at higher concentrations. The explanation for the reduction of the mean chain length during this transition is given below. Consider a system at a ϕ where the surface area is completely filled with trains. If the monomer concentration is increased, more monomers are added to the adsorbed chains due to the favorable u_{LL} interactions. Monomers can be added at the end or in the middle of a train. The latter leads to a bisection of the train, and hence to a shortening of the absorbed chain. Bisection is energetically unfavorable, since an LL pair is lost, but will sometimes occur for entropic reasons. Hence, $\langle N_{ads} \rangle$ decreases with

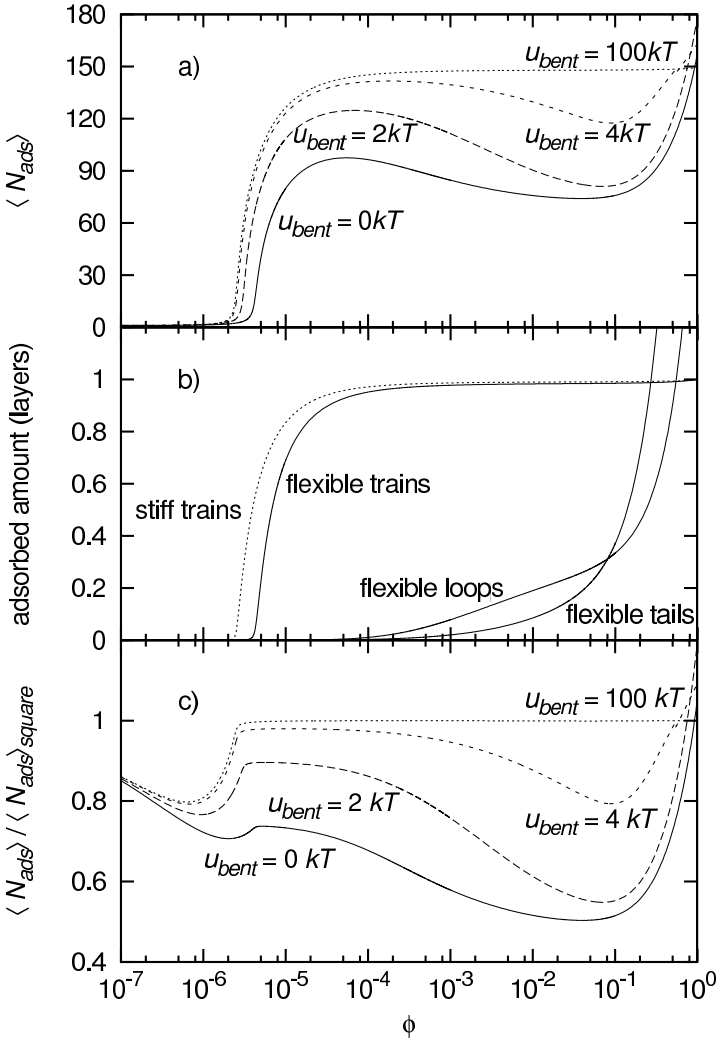

FIGURE 2.3. (a) The dependence of the mean length of adsorbed chains versus ϕ. (b) The total adsorbed amount for various chain substructures, expressed in equivalent lattice layers, depicted on the vertical axis. (c) The quantity shown on the vertical axis is the quotient of $\langle N_{ads} \rangle$ [same quantity as plotted in (a)] and $\langle N_{ads} \rangle_{square}$, which is the mean length calculated with Eq. (2.2) where $q = 4$ and the monomer concentration is the volume fraction of monomers in the layer adjacent to the interface. Parameters: $u_{LL} = -10kT$, $u_{IS} = -4kT$ unless indicated otherwise.

ϕ when chain shortening due to bisections is more important than lengthening of the chains by adding monomers at the ends of the trains.

A comparison between the calculations regarding flexible polymers in Figs. 2.3(a) and 2.3(b) reveals that the sudden increase of the mean length coincides with the filling

of the layer next to the surface, and that the mean length indeed decreases when loops and tails are formed. Figure 2.3(b) shows that stiff polymers adsorb more strongly than flexible monomers, in line with earlier predictions.[17]

The reduction of $\langle N_{ads} \rangle$ is equivalently explained by Eq. 2.2. The chains are confined to the layer next to the surface in the 'train regime' so the adsorbed layer is then effectively a two-dimensional system. When the monomer concentration increases, more tails and loops are formed, so the chains transform into an arrangement of higher dimensionality. Remember that it can be inferred from Eq. (2.2) that the mean length decreases as the dimensionality of the systems increases. This also explains the reduction of the mean length of adsorbed chains at intermediate concentrations. Furthermore, this behavior is not found for stiff supramolecular polymers for that reason. They remain adsorbed as trains at all concentrations so the adsorbed chains remain in a 2-dimensional arrangement. The chain length for adsorbed stiff chains is therefore exactly reproduced by Eq. (2.2) if we choose the occupation of the first layer as the monomer concentration and $q = 4$ which is the coordination number of a square lattice [Fig. 2.3(c)]. It appears from 2.3(a) that $\langle N \rangle$ of adsorbed flexible chains passes a minimum as well and are longer than stiff polymers at very high concentrations. As yet we do not have an explanation for this phenomenon.

The results presented in this chapter describe adsorption that is induced by a favorable energetic interaction between the surface and the indifferent faces of the monomers. Our results for non-zero interaction energy between the linking face and the interface, u_{LS}, are shown in Fig. 2.4. The non-monotonic behavior is still present when the affinity for the surface is identical for linking faces and indifferent faces.

$\langle N_{ads} \rangle$ strongly decreases if u_{LS} is made even more negative, and eventually the maximum disappears altogether (Fig. 2.4). The trains become shorter when u_{LS} becomes more negative because the probability increases that a train ends by means of a linking face pointing towards the surface. Eventually, at $u_{LS} = -\infty$, only dimeric structures at the surface are formed, so $\langle N_{ads} \rangle$ equals 2 in that case.

In conclusion, we have shown that the mean chain length of supramolecular polymers has a non-monotonic concentration dependence in the presence of an adsorbing surface. This phenomenon is caused by a transition from a two-dimensional to a three-dimensional arrangement at the surface. It is to be expected that this behavior is important in experimental systems of supramolecular polymers near interfaces.

The authors acknowledge J. van der Gucht for writing the code that was used to calculate the length distributions from the occupation of lattice sites. H. J. A. Z. would also like to thank C. M. Marques and M. C. P. van Eijk for stimulating discussions related to this work.

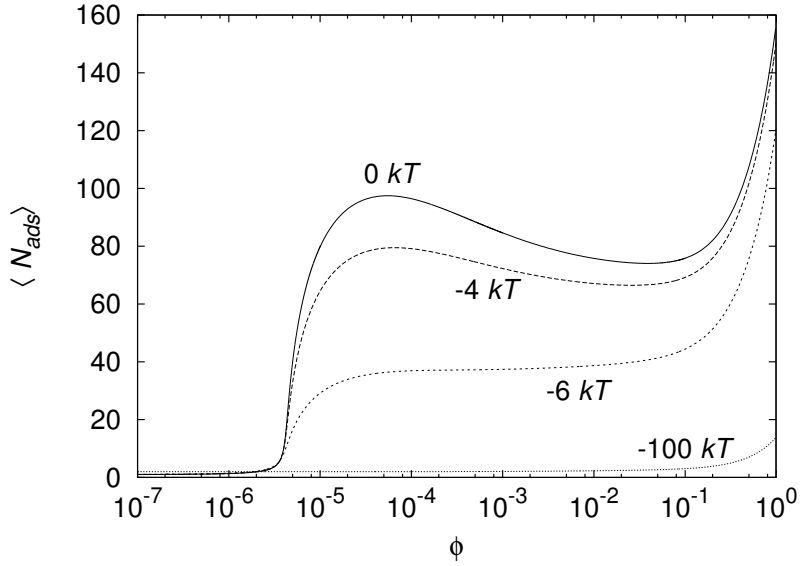

FIGURE 2.4. $\langle N_{ads} \rangle$ is plotted versus the bulk monomer concentration for different values of u_{LS}. $u_{LL} = -10kT$ and $u_{IS} = -4kT$.

References

[1] L. Brunsveld, B. J. B. Folmer, E. W. Meijer, and R. P. Sijbesma, Chem. Rev. **101**, 4071 (2001).
[2] J. van der Gucht, N. A. M. Besseling, and M. A. Cohen Stuart, J. Am. Chem. Soc. **124**, 6202 (2002).
[3] R. S. Scott, J. Phys. Chem. **69**, 261 (1965).
[4] G. Faivre and J.-L. Gardissat, Macromolecules **19**, 1988 (1986).
[5] F. Oosawa and S. Asakura, *Thermodynamics of the Polymerization of Protein*, Academic Press, London, 1975.
[6] M. E. Cates and S. J. Candau, J. Phys.: Condens. Matter **2**, 6869 (1990).
[7] F. Lequeux, Curr. Opin. Coll. Int. **1**, 341 (1996).
[8] V. Schmitt, F. Lequeux, and C. M. Marques, J. Phys. II France **3**, 891 (1993).
[9] P. J. Flory, J. Am. Chem. Soc. **58**, 1877 (1936).
[10] C. C. van der Linden, F. A. M. Leermakers, and G. J. Fleer, Macromolecules **29**, 1172 (1996).
[11] J. van der Gucht and N. A. M. Besseling, Phys. Rev. E **65**, 051801 (2002).
[12] J. van der Gucht and N. A. M. Besseling, J. Phys. Condens. Matter **15**, 6627 (2003).
[13] R. Dickman and C. K. Hall, J. Chem. Phys. **85**, 3023 (1986).
[14] P. Bladon and A. C. Griffin, Macromolecules **26**, 6604 (1993).
[15] J. P. Straley, J. Chem. Phys. **57**, 3694 (1972).
[16] N. A. M. Besseling and J. M. H. M. Scheutjens, J. Phys. Chem. **98**, 11597 (1994).
[17] T. M. Birshtein, E. B. Zhulina, and A. M. Skvortsov, Biopolymers **18**, 1171 (1979).

Chapter 3

Adsorption and Desorption of Reversible Supramolecular Polymers*

Abstract

We report numerical mean-field results on the quasi-chemical level of approximation that describe adsorption of reversible supramolecular polymers at a flat interface. Emphasis is laid on the regime of strong adsorption from a dilute solution. There are two differences with respect to macromolecular polymer adsorption: (i) adsorption sets in at relatively high monomer concentrations of the surrounding solution, and (ii) the surface is filled within a much narrower concentration range. Contrary to macromolecular polymers, supramolecular polymers can therefore be desorbed by dilution of the equilibrium solution by solvent within an experimentally accessible concentration window. Based on simple thermodynamic arguments, we provide a quantitative explanation why supramolecular polymers adsorb at relatively high concentrations. Moreover, we discuss the (by comparison) narrow concentration window wherein filling of the surface occurs. This is attributed to the cooperative nature of supramolecular polymer adsorption. The degree of cooperativity is quantified by means of the Hill parameter n.

3.1. Introduction

Polymers play a central role in molecular biology and are essential in many industrial processes as well. This has contributed to the emergence of various scientific activities to unravel the properties of polymeric compounds since the 1920s. The study of *reversible supramolecular polymers* (also known as *living polymers*) is a relatively recent branch of this diverse field of research. Supramolecular polymers are reversible aggregates consisting of monomers that form linear and/or ring-shaped structures. Solutions of supramolecular polymers usually contain a broad chain length distribution. However, it is not the polydisperse nature as such that sets them apart from regular polymers. Rather, it is their ability to adjust the chain lengths as a response to externally imposed stresses.

Numerous compounds can be classified as "supramolecular polymers." The best studied system is probably cetylammonium bromide, a surfactant that forms semiflexible cylindrical micelles in the presence of sodium or potassium ions.[1, 2] Other examples of compounds that exhibit supramolecular polymer behavior are liquid sulphur,[3]

*Published as: H. J. A. Zweistra and N. A. M. Besseling, Phys. Rev. E **74**, 021806, (2006).

selenium,[4] actin filaments,[5] and specially designed synthetic monomers.[6] The latter group is usually categorized according to the nature of the reversible bond between the monomers:[6] hydrogen-bonded,[7] discotic,[8] and coordination[9] supramolecular polymers. The effort made to produce synthetic supramolecular polymers in recent years has paved the way for validation of many existing theories.

Supramolecular polymers have already surpassed the stage of a mere scientific curiosity or a theorists' toy. They are regarded as highly promising for technological and industrial applications.[6, 10] The possibility to reversibly alter the mean chain length *in situ* (e.g., by applying shear or changing the temperature) makes supramolecular polymers a very promising candidate for numerous applications (e.g., nanotechnology[10]) since the rheological properties of the system can be tuned.

Moreover, polymers in general are very important in inhomogeneous systems, where they are used to control the stabilization of colloidal suspensions,[11] prevent biofouling,[12] etc. By using supramolecular polymers, it is to be expected that the properties of these systems can be adjusted in a more refined way compared to ordinary polymers. It is therefore of interest to predict to what extent supramolecular polymers adsorb to a surface and how they alter the properties of such a surface.

Several studies of supramolecular polymers near nonadsorbing[13–20] and adsorbing[19–21] interfaces were reported in recent years. It was predicted that supramolecular polymers behave more or less similarly to ordinary polymers near interfaces. They are depleted from the interface region for entropic reasons if no favorable energetic interaction occurs for a contact between the polymer and surface. Furthermore, long chains exhibit thicker depletion layers than short chains, which was also predicted for bidisperse classical polymers.[22, 23] Adsorption takes place only when favorable energetic interactions compensate the entropy loss.

All these phenomena are also found in systems that contain ordinary polymers. However, in a recent paper we presented adsorption isotherms from which it can be inferred that for a realistic set of parameters supramolecular polymers may not adsorb unless the volume fraction of monomers in solution is higher than about 10^{-6}.[24] Put in a different way, supramolecular polymers may be desorbed from a surface in that case if the concentration of the surrounding solution is decreased below 10^{-6}, which is well within the experimental range.[25] This behavior is virtually never found for macromolecular polymers, which can normally not be desorbed to a significant extent by just diluting the surrounding solution.[25]

It is to be expected that this profound difference will have important implications in the applicability of supramolecular polymers as surface-modifying agents, because the adsorbed layer can be easily removed by diluting the solution. Since one of the proposed applications of supramolecular polymers is surface modification, it is of interest to study this effect in more detail.

Here we present a systematic study that assesses the effects of varying the model parameters on the adsorption behavior of supramolecular polymers. Previous studies in this field have focused on relatively high concentrations[21] or employed theory that is not particularly well suited to study supramolecular polymers at low concentrations (and hence low aggregation numbers).[19, 20] We will focus on the regime of low monomer concentrations, since this is the relevant regime to study desorption.

Many of the quantitative results presented in this chapter are applicable to the situation where the adsorbed molecules are confined to a thin layer adjacent the surface. This is known as the "train" regime because the adsorbed material resides in trains.[24] This is a relevant regime for desorption, since any layer of adsorbed polymers is flat, provided that the concentration of molecules in the surrounding solution is sufficiently low and adsorption is strong enough. The train regime is especially important when the adsorption contribution per segment is strong. As in our previous paper,[24] we will therefore focus on the strong-adsorbing case.

This chapter is organized as follows. First, the model is described that was used to study the adsorption of supramolecular polymers. Then, in Sec. 3.3, we compare the adsorption isotherms of supramolecular and macromolecular polymers in general terms. Sections 3.4 and 3.5 each address a profound difference in adsorption behavior between the two types of polymer. The chapter is concluded by summarizing the results and providing recommendations for experimental systems (Sec. 3.6).

3.2. Description of the model

We use a cubic lattice model to study the properties of the adsorbed layers of supramolecular polymers in more detail. There are several reasons to choose a discretized model. In comparison with continuum models, lattice models (i) tend to be computationally less demanding, (ii) are easily analyzed, and (iii) allow a very simple and straightforward definition of supramolecular polymers (Fig. 3.1). The main disadvantage of using a lattice model in this case is probably that nematic ordering is not well captured by a discretized approach.[26] However, the focus of this chapter is on flexible chains. It is therefore unlikely that a continuum model would lead to qualitatively different conclusions from those presented in this chapter.

The same model and notation are used in this chapter as in our previous paper.[24] The model is depicted in Fig. 3.1. Molecules are modeled as cubic particles with different faces. Only nearest-neighbor interactions are taken into account. A contact energy is assigned to each pair of faces on adjacent molecules that point toward each other. All energies are given in units of kT for simplicity.

At least two types of interaction energies are present in any system containing adsorbed supramolecular polymers: adsorption energy and linking energy. With adsorption energy we hereby loosely mean the energy difference that a monomer experiences

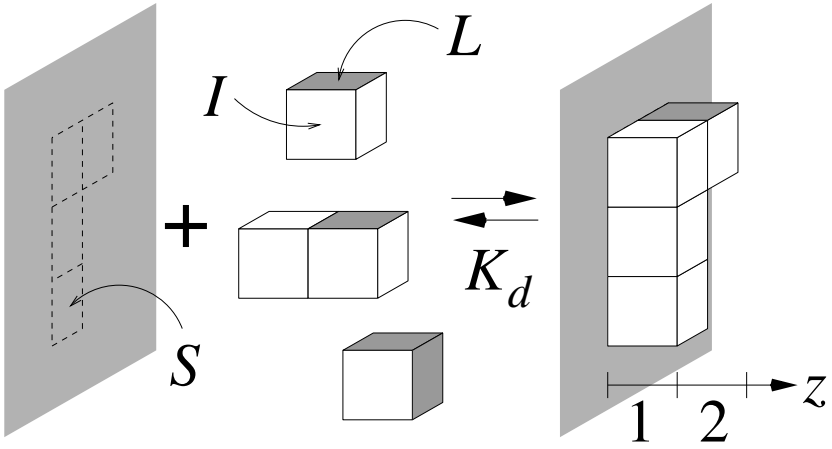

Figure 3.1. Schematic representation of the current model. The supramolecular polymers are modeled as strings of monomers, which are connected by faces of type L (linking faces). Each monomer has exactly two of those faces. The other four faces are of type I (indifferent faces), and we refer to the faces at the surface as S (surface faces). The monomers a and b belong to two different configurations of the monomer because the linking faces are pointing in different directions. The linking faces are perpendicular in molecule a. Hence at a the chain is bent and a is referred to as a "bent" monomer. The linking faces are parallel in molecule b, this is therefore a "linear" monomer. The adsorption of supramolecular polymers is viewed as an equilibrium reaction between the surface and the chains in the bulk. The equilibrium constant of the dissociation reaction is K_d. Solvent molecules (not depicted) are modeled as monomeric, isotropic species without net energetic interaction with monomers or the wall. The spatial coordinate z measures the distance perpendicular to the surface: $z = 1$ next to the surface and z is normalized so that the lattice spacing is equal to unity. The assembly of lattice sites at a certain integer value of z forms a *lattice layer*.

as it is transferred from the bulk to the surface. The adsorption is governed by the parameter u_{IS}, which is the energy that is assigned to each contact between an indifferent face I and the surface S (see Fig. 3.1). In the present study, this energy difference is sufficiently negative; otherwise, the polymers are depleted from the surface.

Moreover, a linking energy u_{LL} is assigned to every contact between two linking faces L (see Fig. 3.1). A reversible bond between two monomers is formed when two linking faces on each monomer are in contact. Therefore u_{LL} may also be seen as the bond energy. The bond energy has to be sufficiently negative for achieving appreciable chain formation. In literature, often the scission energy is used as the parameter that controls chain formation.[1] The scission energy is directly related to u_{LL}: $E_{scission} = -u_{LL}$. Apart from u_{IS} and u_{LL}, all contact energies are set to zero.

We can assign a *bending penalty* u_{bent} to states of monomers where the linking faces are perpendicular with respect to each other. By changing u_{bent}, we can change the flexibility of the polymer chain. It is straightforward to show that the persistence length ℓ_p in a cubic lattice is equal to $\ell_p = 1 + \frac{1}{4}\exp(u_{bent})$.[27, 28] In this chapter, u_{bent} was set to zero (flexible chains) unless stated otherwise.

The internal energy of a system is therefore determined by the occupation of molecules, the orientation of the faces, and the set of energy parameters u_{IS}, u_{LL}, and u_{bent}. These parameters are referred to as a set $\{u\}$. Given $\{u\}$ and the overall monomer concentration ϕ, we must find the distribution of monomers over the system. Grand canonical Monte Carlo simulations could in principle be used to find the occupation of the lattice sites. These calculations yield "exact" results when applied properly. However, it turns out that Monte Carlo methods are unsuitable if realistic bond energies are applied. Realistic bond energies of triple- or quadruple-hydrogen-bonded monomers are in the order of -10 to -20.[6] Such strong interactions lead to excessive equilibration times in Monte Carlo calculations. As in our previous paper, we will therefore use a numerical technique that is virtually unrestricted in parameter choice. By means of this technique, the average occupation of the lattice sites is calculated on the level of the quasi-chemical approximation.[29] Some 20 years ago, it was shown that computations at this level yield far better results in describing the equation of state of chain molecules than random-mixing theories.[30] Yet it can handle very low concentrations and strong interactions while the computational demands remain modest. Since the partition functions and minimization scheme are readily available in literature,[16, 29] they are not repeated here.

It is instructive to compare the properties of reversible supramolecular polymers with irreversibly linked macromolecular polymers. We will use the model proposed by Scheutjens and Fleer to describe adsorbed layers of macromolecular polymers on a mean-field level.[31, 32] We follow the usual notation for macromolecular polymer adsorption in this chapter. The parameter χ is the Flory-Huggins polymer-solvent interaction parameter. The adsorption energy per segment is indicated by χ_s, which is equal to $-u_{IS}$.

3.3. General aspects of adsorption isotherms

In the present quasi-chemical calculation, the surface is infinitely large and completely flat. A chain is adsorbed if at least one monomer of the chain is adjacent the surface. Since a lattice layer represents a certain volume, we can express amounts in terms of equivalent lattice layers. It is convenient to express the adsorbed amounts of monomers in terms of the number of equivalent lattice layers that the monomers of adsorbed chains occupy. Adsorbed amounts are indicated by Γ and can be subdivided in contributions from trains, loops, and tails,[24] denoted as Γ_{tr}, Γ_{lp}, and Γ_{tl}, respectively. The adsorbed amounts plotted against the volume fraction ϕ for a certain choice of parameters $\{u\}$

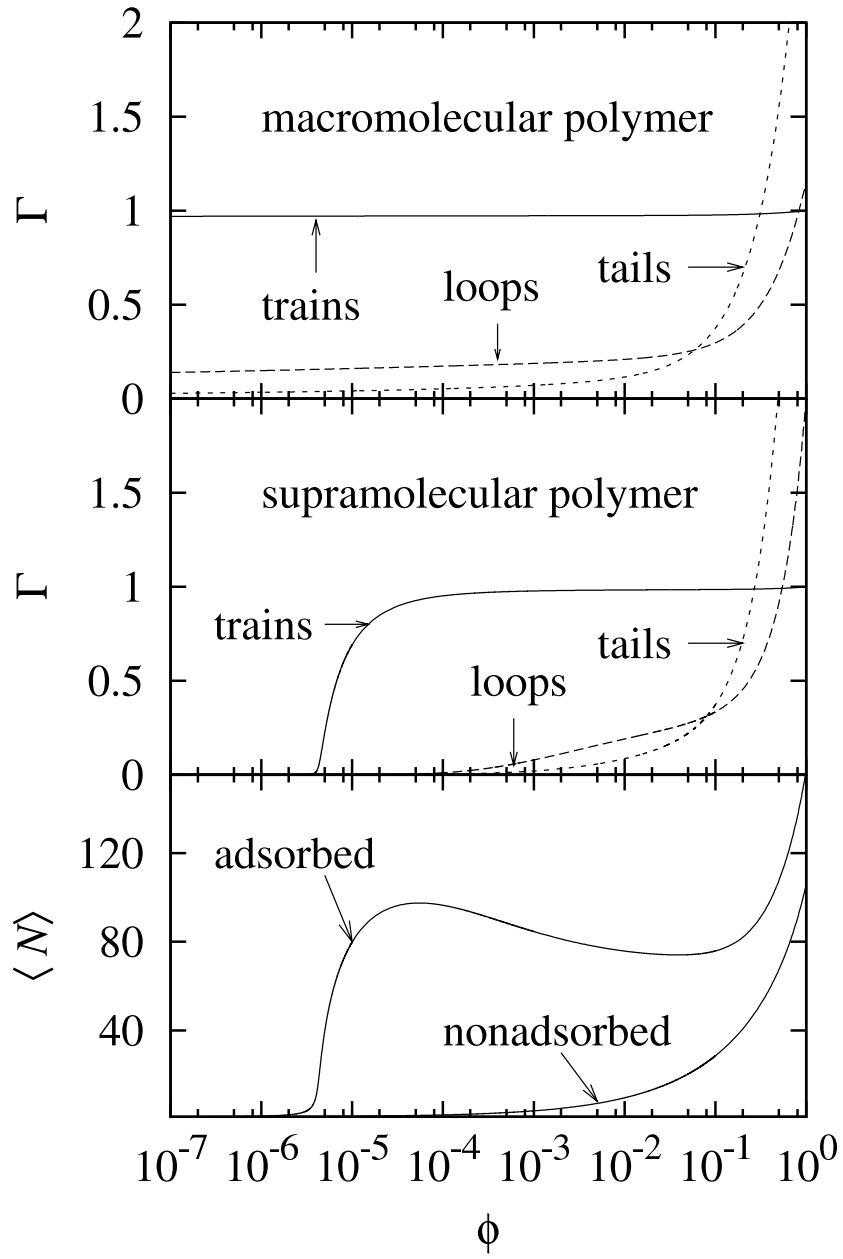

Figure 3.2. The top and the middle plot make a comparison between macromolecular and supramolecular polymers. The adsorbed amounts Γ (expressed in equivalent lattice layers) for trains, loops, and tails are plotted against the volume fraction of monomers in the bulk. The trains are confined to the layer adjacent the interface, so $\Gamma_{tr} \leq 1$. Bottom plot: mean chain length of adsorbed and nonadsorbed supramolecular polymers. The sudden increase in Γ_{tr} coincides with the sudden increase in the mean chain length of adsorbed supramolecular polymers, which indicates cooperativity of the adsorption process. Parameters: $N = 100$, $\chi = 0$, $\chi_s = 4$, $u_{IS} = -4$, $u_{LL} = -10$, and $u_{bent} = 0$.

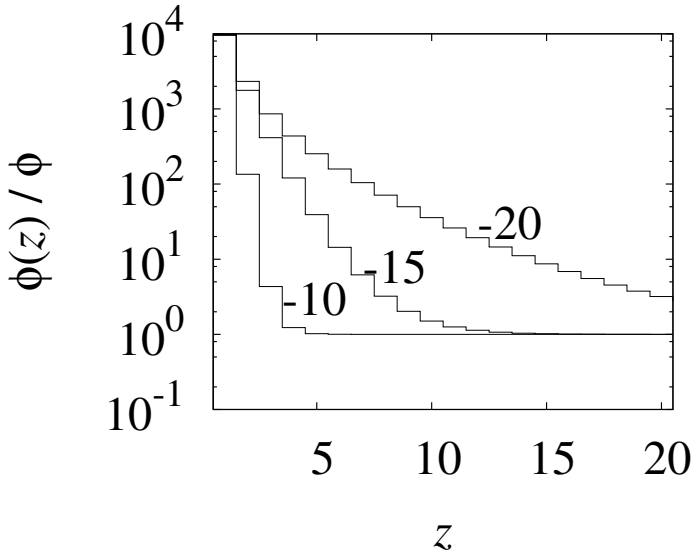

Figure 3.3. Concentration profiles of adsorbed supramolecular polymers for different values of u_{LL}. The ranking number of a layer is indicated by z, where the surface is on the left. The volume fraction of monomers in layer z is denoted $\phi(z)$. Parameters: $\phi = 10^{-4}$ and $u_{IS} = -4$.

are shown in Fig. 3.2. The isotherms shown in this figure more or less reflect the experimental window. The experimentally accessible region of volume fractions has a lower bound at approximately 10^{-8}.[25]

Figure 3.2 compares the adsorption of supramolecular polymers with macromolecular polymers. The adsorption energy per segment is the same in both isotherms. The number of segments of the macromolecular polymer was arbitrarily chosen to match the length of supramolecular polymers in the melt. It was shown previously[16] that the average chain length $\langle N \rangle$ of supramolecular polymers in an isotropic, homogeneous environment is given by

$$\langle N \rangle = 1 + \sqrt{\frac{\phi}{\frac{q}{2} - \phi}} \exp\left(-\frac{u_{LL}}{2}\right), \tag{3.1}$$

where q is the coordination number of the lattice ($q = 6$ for a cubic lattice). Equation (3.1) is exact within the quasi-chemical approximation. In a polymer melt, $\phi \approx 1$; hence, $\langle N \rangle$ is then about 100 for the supramolecular polymers shown in Fig. 3.2. Therefore the isotherm was compared with macromolecular polymers of length 100.

Supramolecular polymers display adsorption behavior which is in a number of respects similar to macromolecular polymers. Trains dominate at low ϕ, and at increasing ϕ first loops are formed, but eventually, at very high concentrations, most of the adsorbed material resides in tails.

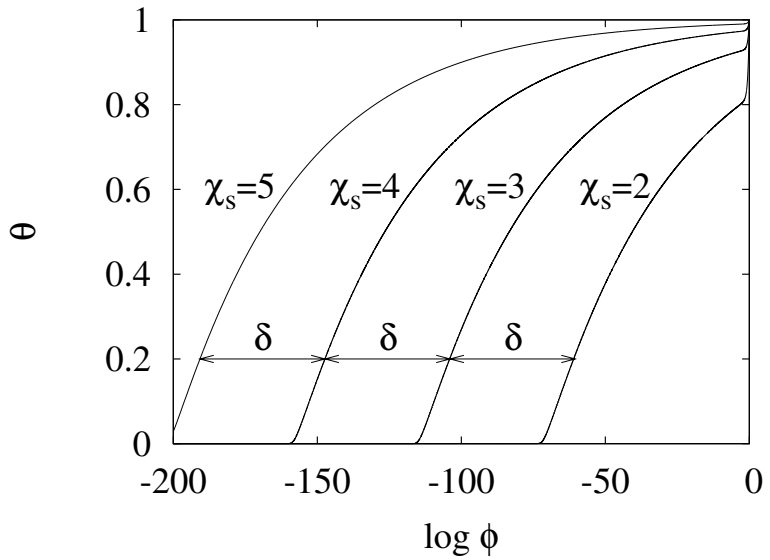

Figure 3.4. Adsorption isotherms of macromolecular polymers at different adsorption energies χ_s. Parameters: chain length $N = 100$, $\chi = 0$, cubic lattice. A different value of χ_s leads to a shift of the isotherm of magnitude $\delta = \Delta \log \phi$. The shift was calculated according to $\delta = N\Delta\chi_s / \ln 10$, which assumes strong adsorption.

However, there are two notable differences between the two isotherms shown in Fig. 3.2. First, at low ϕ loops are far more prominent for macromolecular polymers than for supramolecular polymers. This is due to the decrease in chain length of supramolecular polymers upon decreasing ϕ: Eq. (3.1) shows that the chain length decreases with decreasing concentration. When stronger bonds are formed (u_{LL} more negative), then more extended layers are formed, as is demonstrated in Fig. 3.3.

The second difference between the isotherms in Fig. 3.2 is that macromolecular polymers fill almost the entire surface in the entire shown concentration range whereas supramolecular polymers show a buildup of the train fraction only above $\phi = 10^{-5}$ (for this set of model parameters). These results indicate that supramolecular polymers can be desorbed by diluting the solution which is in contact with the surface. To remove macromolecular polymers in this way is very difficult, as was already pointed out by Scheutjens and Fleer in the 1980s.[33]

Let us determine how difficult it actually is to desorb macromolecular polymers. For sufficiently low concentrations, adsorbed polymers always consist completely of trains. When one is interested in removing the adsorbed amount entirely, it is imperative to study the train regime. Hence it is sufficient to characterize adsorption by simply the *surface coverage* $\theta \equiv \Gamma_{tr}$. The parameter θ is equal to the volume fraction of monomers at $z = 1$. Throughout the rest of this chapter, we will refer to plots of θ versus ϕ as "adsorption isotherms."

Adsorption isotherms of macromolecular polymers for several values of χ_s are shown in Fig. 3.4. This plot illustrates that macromolecular polymers desorb only at excessively low concentrations.

The part of the isotherm that is of most interest is the region where the surface sites become occupied to an appreciable extent. We loosely denote this process as "filling of the surface." Filling of the surface to a appreciable extent requires a change of monomer concentration of many decades in the case of macromolecular polymers, but less than one decade for adsorbing supramolecular polymers.

A physical explanation for this phenomenon is cooperativity: adsorbing supramolecular chains do not only profit from IS interactions, but also from forming bonds with chains that are already present at the surface. Therefore the increase in Γ_{tr} in Fig. 3.2 coincides with a large increase in the mean chain length of adsorbed supramolecular polymers. This effect was already observed previously for supramolecular polymers studied by means of an analytical[20] and numerical[24] self-consistent field theory. As a result, adsorption of supramolecular polymers is *enhanced* by the presence of already adsorbed molecules, whereas the adsorption of macromolecular polymers is *hampered* by adsorbed polymers.

Summarizing this section, we state that in comparison with macromolecular polymers, the adsorption isotherms of supramolecular polymers (i) are shifted due to a change in adsorption energy per segment much less along the concentration axis and (ii) exhibit a much steeper increase in θ due to the cooperative nature of adsorption. These effects will be discussed separately in the following sections.

3.4. Isotherm shift along the concentration axis

The purpose of this section is to give an explanation why supramolecular polymers can be desorbed within experimentally accessible concentrations, whereas this is almost impossible for macromolecular polymers. Adsorption isotherms $\theta(\phi)$ of macromolecular polymers for different adsorption energies are shown in Fig. 3.4. A few adsorption isotherms of supramolecular polymers are shown in Fig. 3.5. Varying χ_s or $\{u\}$ does not change the shape of the adsorption isotherm, but leads to a *shift* of the isotherm along the $\log \phi$ axis.

The magnitude of this shift $\delta = \Delta \log \phi$ can be found by the consideration that the populations of molecules at the surface and in solution are distributed according to a Boltzmann equilibrium:

$$\frac{\theta}{\phi(\theta)} = e^{-\Delta_{ads}F}, \tag{3.2}$$

where $\phi(\theta)$ is the monomer concentration in the bulk solution in equilibrium with a surface with surface coverage θ. In Eq. (3.2), $\Delta_{ads}F$ is the free energy of adsorption per molecule: $\Delta_{ads}F = \Delta_{ads}U - T\Delta_{ads}S$, where $\Delta_{ads}U$ and $\Delta_{ads}S$ are the changes

in molecular energy and entropy upon adsorption. It is not easy to obtain analytical expressions for $\Delta_{ads}S$. In the case of macromolecular polymers, $\Delta_{ads}S$ is a nontrivial function of ϕ, N and θ. However, $\Delta_{ads}U$ is easily found. For macromolecular polymers, $\Delta_{ads}U = -N\chi_s$,[34] since we are considering athermal chains in the regime where the chains adsorb as trains. Furthermore, we can neglect the ϕ dependence of $\Delta_{ads}S$ since the monomer concentrations needed to desorb polymers are generally so low that the molecules in the bulk solution are effectively noninteracting. Hence it follows from Eq. (3.2) that:

$$\ln \phi(\theta) = -N\chi_s + f_0(N, \theta), \tag{3.3}$$

where $f_0(N, \theta)$ is some nontrivial function that depends on N and θ. Equation (3.3) shows that varying χ_s results in a shift of the adsorption isotherm along the $\ln \phi$ axis. The shift of the adsorption isotherm in Fig. 3.4 is very well predicted by Eq. (3.3). Furthermore, the shift is proportional to N, which means that it is very hard to desorb macromolecular polymers of considerable length.

Let us compare this result with the shift of adsorption isotherms for supramolecular polymers. We start from the same Boltzmann equilibrium as in Eq. (3.2), but now we separate $\Delta_{ads}F$ into a part that depends on the model parameters and a part that depends solely on θ: $\Delta_{ads}F = \Delta_{ads}F(\{u\}) + \Delta_{ads}F(\theta)$. Note that here $\Delta_{ads}F$ is the adsorption energy per monomer. It follows from Eq. (3.2) that

$$\ln \phi(\theta) = \Delta_{ads}F(\{u\}) + f_0(\theta), \tag{3.4}$$

where $f_0(\theta)$ is some nontrivial function that depends on θ. The main contribution to $f_0(\theta)$ is the entropy loss when a monomer is moved from the bulk to the surface region. Analytical expressions for $f_0(\theta)$ are not available, but again $\Delta_{ads}F(\{u\})$ is tractable. It is separated according to the three interaction types, $\Delta_{ads}F(\{u\}) = \Delta_{ads}F(u_{LL}) + \Delta_{ads}F(u_{IS}) + \Delta_{ads}F(u_{bent})$, and each of these three components can be calculated separately.

Adsorption isotherms of supramolecular polymer adsorption with varying $\{u\}$ are shown in Fig. 3.5. For a typical adsorption isotherm as described in Fig. 3.5, for example $u_{LL} = -10$, $u_{IS} = -6$, the filling of the surface occurs when $\phi \approx 10^{-6}$. At this concentration, $\langle N \rangle \approx 1.09 \approx 1$ according to Eq. (3.1). This means that the adsorbed monomers at the surface are in equilibrium with a solution that consists almost exclusively of solvent molecules and single monomers. The reaction is therefore associated with the formation of a single IS contact. Furthermore, it is very likely that a monomer adsorbs next to a monomer that is already present at the surface, due to the high binding energy. Therefore $\Delta_{ads}F(u_{LL}) = u_{LL}$ and $\Delta_{ads}F(u_{IS}) = u_{IS}$. The shift in Figs. 3.5A and 3.5B are therefore $\delta = \Delta u_{LL}/\ln 10$ and $\delta = \Delta u_{IS}/\ln 10$, respectively. The large prefactor N in Eq. (3.3) for macromolecular polymers is missing for supramolecular polymers. We return to this point below.

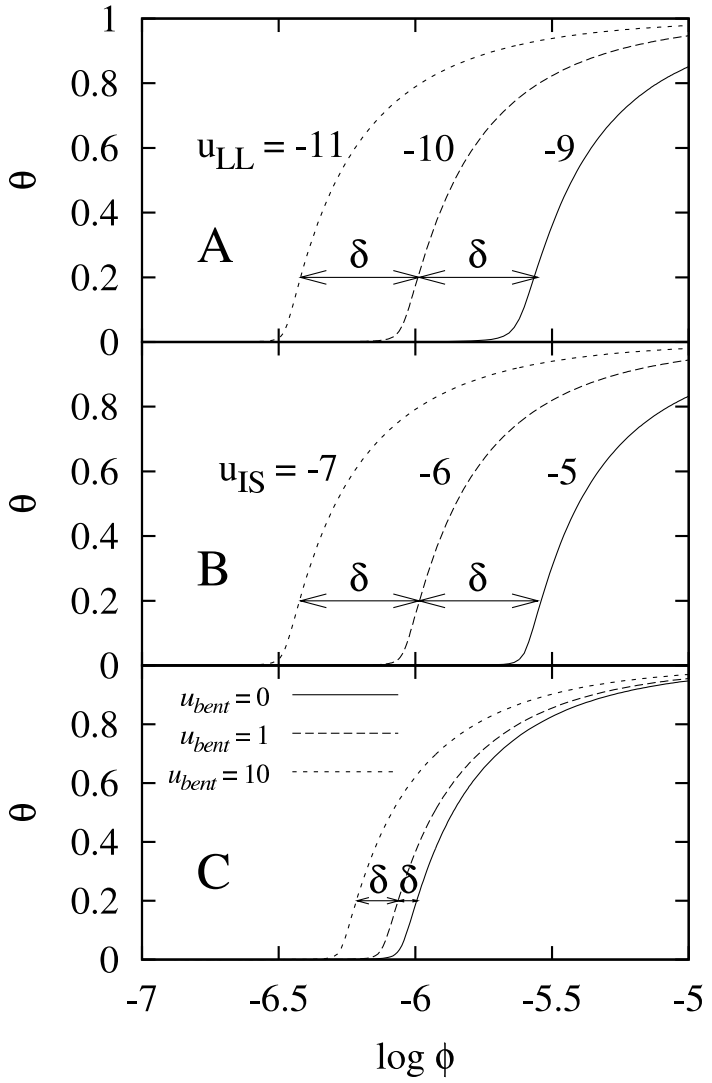

Figure 3.5. Adsorption isotherms of supramolecular polymer solutions: plot of surface coverage θ versus monomer concentration in the bulk solution ϕ. Plot A: effect of bond energy. Parameters: $u_{IS} = -6$, $u_{bent} = 0$; u_{LL} is varied. Plot B: effect of adsorption energy. Parameters: $u_{LL} = -10$, $u_{bent} = 0$; u_{IS} is varied. Plot C: effect of flexibility of the chain. Parameters: $u_{IS} = -6$, $u_{LL} = -10$; u_{bent} is varied. The shifts of the adsorption isotherms, indicated by $\delta = \Delta \log \phi$, were calculated by means of Eqs. (3.4) and (3.7).

The quantity $\Delta_{ads}F(u_{bent})$ is calculated as

$$\Delta_{ads}F(u_{bent}) = -\ln \frac{Q^{mon}_{surf}}{Q^{mon}_{bulk}}, \tag{3.5}$$

where Q_{surf}^{mon} and Q_{bulk}^{mon} are the canonical partition functions of a single monomer at the surface and in the bulk solution. In the present lattice model, a monomer in the bulk is free to position one linking face in any of the q directions. The other linking face is to be placed on 1 of the $(q-1)$ remaining directions of which $(q-2)$ correspond to a bent state (with associated Boltzmann weight $\exp(-u_{bent})$) and only one corresponds to a linear state. Hence, $Q_{bulk}^{mon} = q\left((q-2)\exp\left(-u_{bent}\right)+1\right)$.

For the computation of Q_{surf}^{mon}, we neglect the configurations where one of the linking faces is in contact with the surface. This is reasonable for most situations where u_{IS} or u_{LL} is sufficiently negative. It is easily shown that for our model $Q_{surf}^{mon} = 4\left(2\exp\left(-u_{bent}\right)+1\right)$ and hence that

$$\Delta_{ads}F(u_{bent}) = \ln\frac{6(4\exp\left(-u_{bent}\right)+1)}{4(2\exp\left(-u_{bent}\right)+1)}. \tag{3.6}$$

The shift of the isotherm with varying u_{bent} is quantified by Eq. (3.6), as shown in Fig. 3.5.

For completely flexible chains, $\exp(-u_{bent}) = 1$, and for rods, $\exp(-u_{bent}) = 0$; therefore, $\Delta_{ads}F(u_{bent})$ is at least $\ln 3/2 \approx 0.405$ (stiff chains) and at most $\ln 5/2 \approx 0.916$ (completely flexible chains). The entropy penalty of adsorption is less for stiff chains than for flexible chains since stiff chains lose less configurational entropy. This effect is already discussed in detail for semiflexible polymers.[35]

In conclusion, we have found that $\Delta_{ads}F(\{u\})$ can be constructed as follows:

$$\Delta_{ads}F(\{u\}) = u_{LL} + u_{IS} + \ln\frac{6(4\exp\left(-u_{bent}\right)+1)}{4(2\exp\left(-u_{bent}\right)+1)}. \tag{3.7}$$

Equations (3.4) and (3.7) describe the magnitude of a shift $\Delta\ln\phi$ as a result of a change in $\{u\}$ quantitatively. We can therefore find any adsorption isotherm in the regime of strong adsorption from a dilute solution if only one is known.

For our present model, the contribution of chain stiffness to ΔF_{ads} by increasing the stiffness of the chains is at most $\ln 5/3 \approx 0.5$. However, note that nematic ordering of the chains within the plane parallel to the surface is ignored on the present level of approximations. Taking nematic ordering into account would not necessarily lead to accurate results due to lattice artifacts.[26] Therefore the case that the monomers are very stiff may not be accurately described by the present treatment, and from now on we will focus exclusively on completely flexible chains.

The range of validity of Eq. (3.7) is demonstrated in Fig. 3.6. Equation (3.7) is valid when $\langle N\rangle \approx 1$ at concentrations where filling of the surface occurs. This is the regime where both u_{LL} and u_{IS} are sufficiently negative. In this regime, changing the adsorption energy has exactly the same effect on adsorption as changing the linking energy. Since the shape of the adsorption isotherm on a logarithmic ϕ scale is virtually unaffected by a change in either u_{LL} or u_{IS}, we can specify the shift of the isotherm

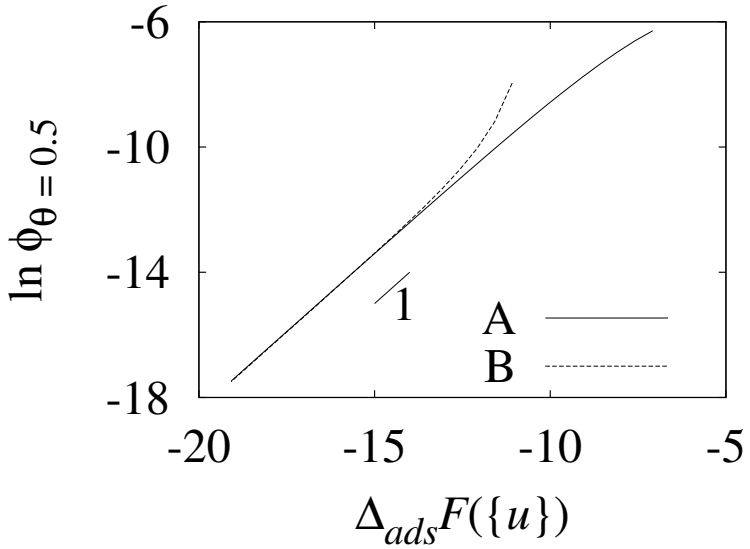

Figure 3.6. This plot shows $\ln \phi_{\theta=0.5}$ versus $\Delta_{ads}F(\{u\})$ to illustrate the relation between $\Delta_{ads}F(\{u\})$ and the shift of the adsorption isotherms. The quantity $\phi_{\theta=0.5}$ is the overall monomer concentration at which $\theta = 0.5$. Equation (3.7) with $u_{bent} = 0$ was used to calculate $\Delta_{ads}F(\{u\})$. Plot A: effect of bond energy: $u_{IS} = -6$; u_{LL} is varied. Plot B: effect of adsorption energy: $u_{LL} = -10$; u_{IS} is varied. Equation (3.4) predicts a slope of unity for this plot.

by comparing values of ϕ for a given θ. This is demonstrated in Fig. 3.6, for the case $\theta = 0.5$, where plot A and plot B of Fig. 3.6 merge for low ΔF_{ads}. Deviations from slope 1 are found when u_{LL} or u_{IS} becomes less negative since then the adsorbed layer is not limited to the lattice layer next to the surface. The description given in this section therefore breaks down when the linking energy or the adsorption energy is not strong enough.

At this point, we compare the magnitudes of the shift in the adsorption isotherms for macromolecular polymers (Fig. 3.4) and supramolecular polymers (Fig. 3.5). For supramolecular polymers, we find that the isotherm shift associated with a change of the adsorption energy is in the present regime $\Delta \ln \phi = \Delta u_{IS}$ whereas for macromolecular polymers, $\Delta \ln \phi = -N\Delta\chi_s = N\Delta u_{IS}$. In other words, if the change in adsorption energy per segment is the same, then the isotherms of macromolecular polymers are shifted N times more than isotherms of supramolecular polymers. Adsorption and desorption of supramolecular polymers occur within an experimentally accessible concentration window. In the case of macromolecular polymer adsorption, the part of the isotherm where filling of the surface occurs is shifted out of the experimental range due to the large prefactor N.

Table 3.1. Values of $\phi_{\theta=0.9}/\phi_{\theta=0.1}$, which is a measure of the steepness of the adsorption isotherm, for several types of polymer. Parameters: $u_{LL} = -10$, $u_{IS} = -4$, $\chi_s = 4$, and $\chi = 0$.

Polymer		$\phi_{\theta=0.9}/\phi_{\theta=0.1}$
Supramolecular		6.4
Macromolecular	$N = 100$	6.7×10^{95}
	$N = 50$	2.4×10^{48}
	$N = 10$	2.6×10^{10}

3.5. Cooperativity of adsorption

In the previous section, it was shown that the adsorption isotherms of supramolecular polymers are shifted along the $\ln \phi$ axis as a result of changing the adsorption energy to a much lesser extent than macromolecular polymers. This is necessary but not sufficient for desorption of supramolecular polymers to take place within the experimental range of monomer concentrations. Another requirement is that desorption takes place within a narrow concentration range. Let us arbitrarily define a θ interval where filling of the surface occurs, $0.1 < \theta < 0.9$, and compare the monomer volume fractions at both ends of this interval. The quotient $\phi_{\theta=0.9}/\phi_{\theta=0.1}$ is a measure for the range of volume fractions in which the surface is filled. Several values of $\phi_{\theta=0.9}/\phi_{\theta=0.1}$ for a supramolecular polymer and macromolecular polymers of three chain lengths are given in Table 3.1. In the case of supramolecular polymers, reducing the surface coverage from 0.9 to 0.1 requires reducing the monomer concentration by a factor of about 6. By contrast, for macromolecular polymers of length 100, reducing the surface coverage by the same amount demands a decrease of the concentration by almost 100 *decades*. The range reduces with decreasing N but is still 10 decades wide if $N = 10$, which is very short for polymeric standards.

The physical background of this remarkable difference is cooperativity of adsorption in the case of supramolecular polymers but not in the case of macromolecular polymers. Unlike macromolecular polymers, adsorbing supramolecular chains not only profit from the adsorption energy, but also from favorable interactions with other monomers that are already present at the surface. Since adsorption is enhanced as more monomers adsorb to the surface, it is a *cooperative* process. It would be interesting to try to quantify the degree of cooperativity of polymer adsorption and to compare the degrees of cooperativity for covalent and reversible polymers.

Cooperativity is a widespread notion in quantitative biochemistry and can be quantified by the formalism developed by Hill. The Hill theory was originally formulated to explain the sigmoidal binding curve of oxygen to hemoglobin.[36] This protein has four oxygen-binding sites, but this fact alone is not sufficient to explain the sigmoidal shape

of the binding curve. Hill described dissociation of a oxygen-hemoglobin complex by a dissociation constant

$$K_{Hill} = \frac{[P][L]^n}{[PL_n]}, \tag{3.8}$$

where P and L indicate protein and ligand, and square brackets denote concentration. Individual protein molecules may differ in the number of bound oxygen molecules. Hence n in Eq. (3.8) is in general not an integer.

The parameter n is known as the Hill coefficient, and it is a measure for the degree of cooperativity of the reaction. If there is no cooperativity, n is equal to unity. In the case of positive cooperativity, $n > 1$, which means that binding is enhanced when more ligands are bound to the protein. On the other hand, $n < 1$ denotes negative cooperativity.

We use this concept to quantify the degree of cooperativity of polymer adsorption. It is possible to view the adsorption of polymers as an equilibrium reaction between parts of a surface S and a number of bulk chains indicated by B:

$$S + nB \leftrightarrows SB_n.$$

Here S is a part of a surface that can accomodate B_n. The dissociation equilibrium constant of this reaction is

$$K_d = \frac{[S][B]^n}{[SB_n]}. \tag{3.9}$$

The Hill coefficient n is the central parameter to describe cooperativity of polymer adsorption in the present formulation. The quantity $[B]$ is the number concentration of chains in solution. For macromolecular polymer adsorption, $[B] = \phi/N$; for supramolecular polymers, $[B] = \phi/\langle N_b \rangle$, where $\langle N_b \rangle$ is found by means of Eq. (3.1).

As in the previous sections, we focus on the case that only trains are adsorbed. We write the saturation of the surface region θ as

$$\theta = \frac{[SB_n]}{[SB_n] + [S]} = \frac{[B]^n}{[B]^n + K_d}. \tag{3.10}$$

We can calculate n for the supramolecular adsorption by linearizing Eq. (3.10) according to

$$\log \frac{\theta}{1-\theta} = n \log[B] - \log K_d. \tag{3.11}$$

The Hill coefficient n can be found by determining the slope of the plot of $\log \theta/(1-\theta)$ against $\log[B]$. Such a plot is known as a *Hill plot*.

Hill plots of supramolecular polymers (curve I) and nonassociating (curve II) and nonadsorbing (curve III) monomers are shown in Fig. 3.7. The adsorption isotherms (not shown) of all three compounds merge when $\phi \to 1$ because the effect of contact energies vanishes in the melt.[25] Curves I and III in Fig. 3.7 merge at high $[B]$ because the mean chain length in solution is the same for both monomers. Curves I and II merge at low $[B]$ because monomers adsorb individually at very low concentrations

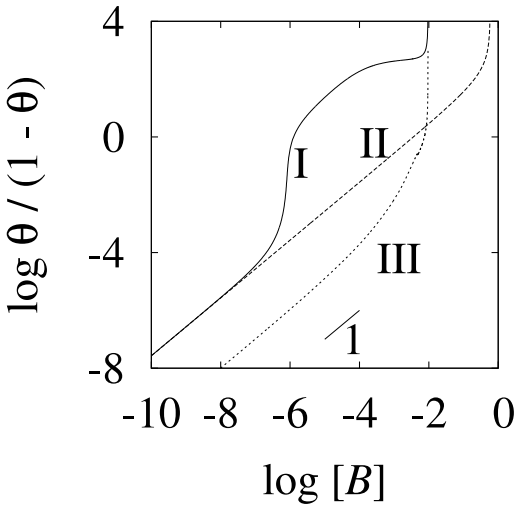

Figure 3.7. Hill plots: plot of $\log \frac{\theta}{1-\theta}$ versus $\log[B]$, where $[B]$ is the number concentration of chains. It is inferred from Eq. (3.11) that the slope of this graph is equal to n, which is a measure for the degree of cooperativity of the adsorption. Curve I: supramolecular polymers. Parameters: $u_{IS} = -6$, $u_{LL} = -10$. Curve II: nonassociating, adsorbing monomers. Parameters: $u_{IS} = -6$, $u_{LL} = 0$. Curve III: associating monomers without affinity for the surface region. Parameters: $u_{IS} = 0$, $u_{LL} = -10$.

where $\langle N \rangle \approx 1$. We expect to find cooperative adsorption only when both u_{LL} and u_{IS} are negative. Indeed, the slopes of curves II and III are unity (except at very high concentrations), which indicates no cooperativity. On the other hand, the region in curve I around $[B] \approx 10^{-6}$ has a slope much larger than 1, indicating positive cooperativity.

Curve I in Fig. 3.7 has clearly a nonuniform slope, which means that n depends on θ. This dependence is shown in Figs. 3.8 and 3.9. At very low surfaces coverages, n is equal to unity. This is the Henryregime, where the adsorbed molecules are far apart and do not interact with each other. As θ increases, n exhibits a sharp increase with θ (Fig. 3.9). This indicates that adsorption in this region is strongly enhanced by the presence of other monomers. At a certain point, n starts to decrease with θ because it becomes more difficult to adsorb more monomers due to excluded volume interactions. Still, n remains larger than unity throughout most of the isotherm where filling of the surface occurs.

It is of interest to assess the effect of $\Delta_{ads}F(\{u\})$ on the degree of cooperativity. Since n is strongly dependent on θ, it is necessary to compare values of n at a specific θ. We choose arbitrarily to compare values at $\theta = 0.5$. The plot of $n_{\theta=0.5}$ versus $\Delta_{ads}F(\{u\})$ is shown in Fig. 3.10. Perhaps surprisingly, $n_{\theta=0.5}$ reaches a plateau for strong adsorption.

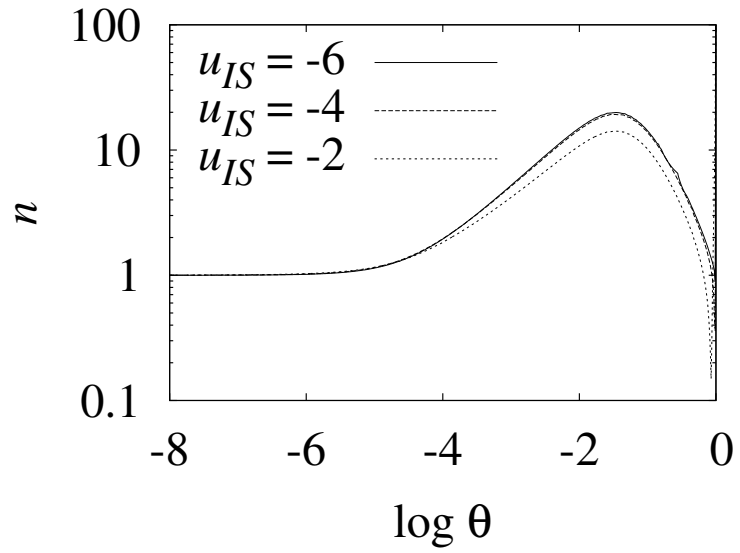

FIGURE 3.8. The slope of the Hill plot, the Hill coefficient n, is plotted against the logarithm of the surface coverage θ for different values of the adsorption energy u_{IS}. The bond energy was -10.

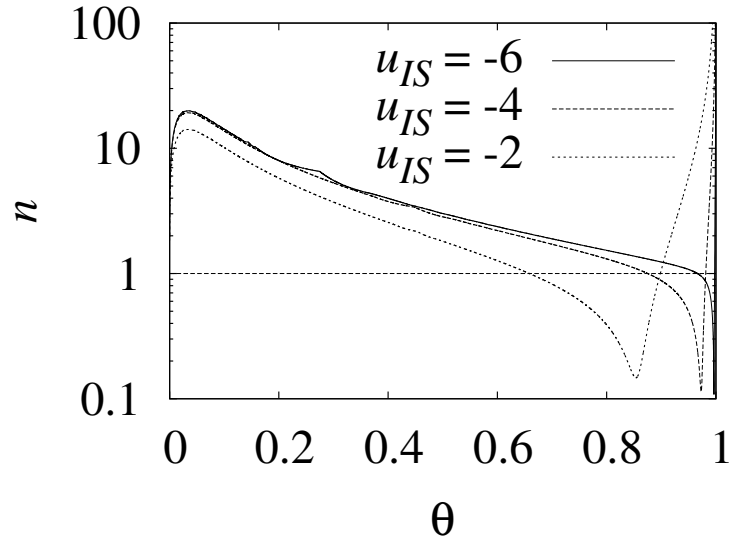

FIGURE 3.9. As in Fig. 3.8, except θ is plotted on a linear scale.

Apparently, the degree of cooperativity is independent of the strength of adsorption in that region. The origin of this effect can be deduced from an observation made in Sec. 3.4: namely, that the adsorption isotherms are merely shifted along the $\ln \phi$ axis at a different $\Delta_{ads}F(\{u\})$. The Hill coefficient n is the slope of the Hill plot; therefore,

$$n = \frac{d \ln \frac{\theta}{1-\theta}}{d \ln \frac{\phi}{\langle N \rangle}}. \tag{3.12}$$

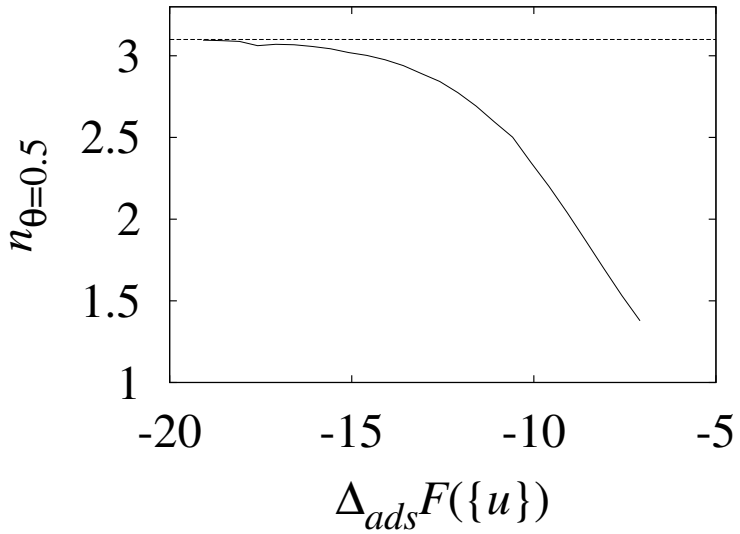

Figure 3.10. Dependence of $n_{\theta=0.5}$ on $\Delta_{ads}F(\{u\})$, where $n_{\theta=0.5}$ is n at $\theta = 0.5$ and $\Delta_{ads}F(\{u\})$ is calculated according to Eq. (3.7). Parameters: $u_{IS} = -6$; u_{LL} was varied. The maximum value of $n_{\theta=0.5}$ (shown as a dashed line) can be computed from the adsorption isotherms by means of Eq. (3.13).

Since $\langle N \rangle$ is equal to unity to a very good approximation in this regime, this is equivalent to

$$n = \frac{1}{\theta\,(1-\theta)} \frac{d\theta}{d\ln\phi}, \tag{3.13}$$

where the differential quotient on the right-hand side of Eq. (3.13) is recognized as the slope of the adsorption isotherm plotted on a logarithmic scale. The slope of the adsorption isotherms at a certain θ is the same for each value of $\Delta_{ads}F(\{u\})$. Therefore n does not increase indefinitely with decreasing $\Delta_{ads}F(\{u\})$.

Summarizing, it was shown that $n > 1$ for strongly adsorbing supramolecular polymer throughout the (arbitrary) range $0.1 < \theta < 0.9$. Let us compare this with macromolecular polymer adsorption. Several Hill plots of macromolecular polymer adsorption are depicted in Fig. 3.11. These plots are quite similar to adsorption isotherms plotted double logarithmically–for example Ref.[33] At low concentrations, a Henry regime is observed. At higher concentrations (but still well below the experimental range) a crossover to a pseudoplateau region is found.

The slopes of the Hill plots are shown in Figs. 3.12 and 3.13. The plots merge at $\phi \to 1$, since the value of χ_s is irrelevant in a polymer melt. Like the Hill plots of supramolecular polymers, $n = 1$ at very low θ. However, n starts to decrease already at a surface coverage of less than 1%, indicating *negative* cooperativity over the entire range $0.1 < \theta < 0.9$ for strongly adsorbing polymers. The physical background is obviously excluded volume interactions. In conclusion, a dramatic difference in the

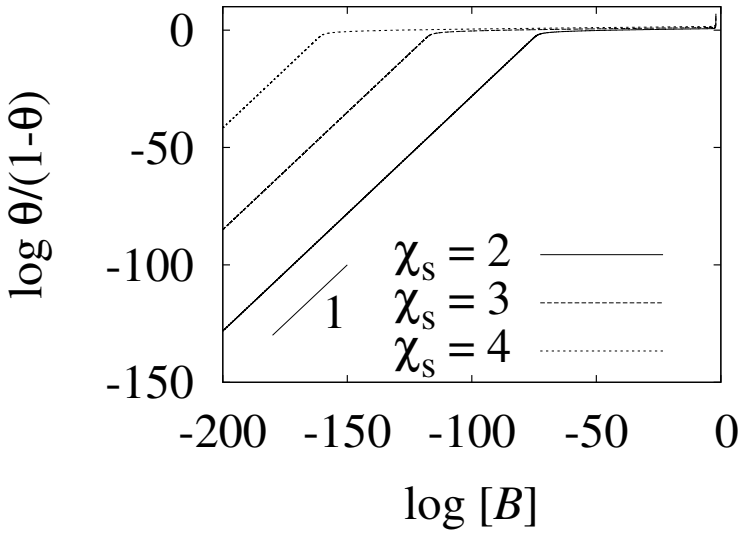

Figure 3.11. Hill plots of macromolecular polymer adsorption for different values of χ_s.

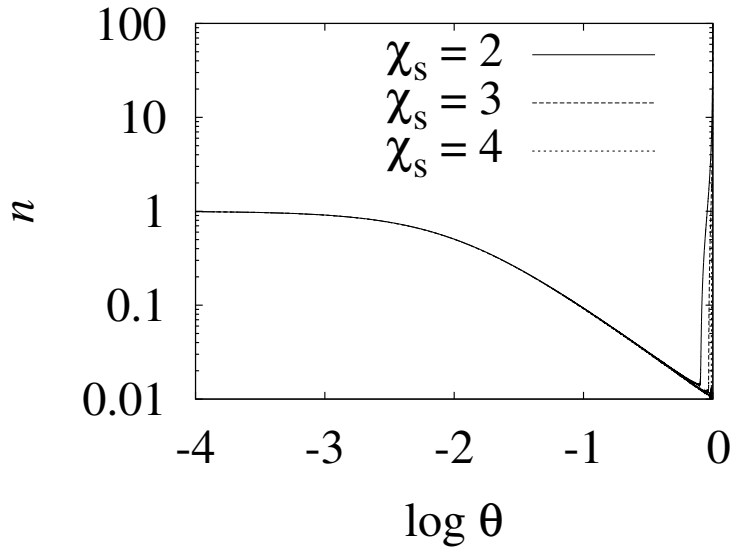

Figure 3.12. Dependence of n on $\log\theta$ for macromolecular polymers for different adsorption energies χ_s. Parameters: chain length $N = 100$, $\chi = 0$.

cooperativity of adsorption is observed. These results give at least a qualitative explanation for the enormous difference in $\phi_{\theta=0.9}/\phi_{\theta=0.1}$ between supramolecular polymers and macromolecular polymers.

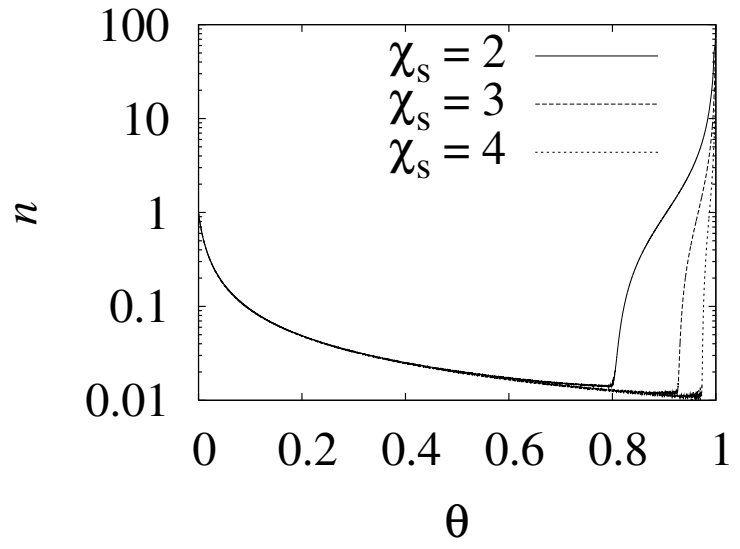

Figure 3.13. As in Fig. 3.12 but now θ is plotted on a linear scale.

3.6. Conclusion

In this chapter, a comparison is made between adsorption of supramolecular polymers and macromolecular polymers. It is found that supramolecular polymers can be desorbed by dilution while this is nearly impossible for high-molecular-weight macromolecular polymers. Two differences between the adsorption isotherms of supramolecular polymers and macromolecular polymers contribute to this discrepancy: in comparison with macromolecular polymer adsorption, adsorption of supramolecular polymers generally occurs at much higher monomer concentrations and within a much narrower concentration range.

We performed numerical calculations to obtain adsorption isotherms of macromolecular and supramolecular polymers in the regime of strong adsorption from dilute solution. Although it is not possible to find an analytical expression for the shape of the isotherms, it is possible to formulate relatively simple expressions for the *shift* of the isotherm along the $\ln \phi$ axis as a result of a change in the adsorption energy per segment u_{LL}. This shift $\Delta \ln \phi$ is equal to $\langle N \rangle u_{LL}$, where $\langle N \rangle$ is the average number of segments per chain in the surrounding solution. For supramolecular polymers, $\langle N \rangle$ decreases with decreasing concentration. In the regime that we studied, $\langle N \rangle \approx 1$ in the part of the isotherm where filling of the surface takes place. By contrast, $\langle N \rangle$ of macromolecular polymers is generally large and independent of concentration. The shift of the adsorption isotherms by changing u_{LL} is therefore much more pronounced for macromolecular polymers than for supramolecular polymers. As a result, the part of the isotherm where filling of the surface occurs is beyond the experimental range for macromolecular polymers.

The second important difference between adsorption of macromolecular polymers and supramolecular polymers is the concentration range in which filling of the surface occurs. This takes many decades of concentration in the case of macromolecular polymers, but generally only one decade for supramolecular polymers. This difference is due to the cooperative nature of supramolecular polymer adsorption: up to a certain θ, adsorption is enhanced as more monomers adsorb to the surface except at extremely low values of θ. The cooperative nature is analyzed by applying the Hill theory to polymer adsorption. The cooperativity parameter is the Hill coefficient n. If $n > 1$, then positive cooperativity is observed and $n < 1$ in the case of negative cooperativity.

Polymers adsorb as individual molecules in the Henry regime. Therefore $n = 1$ at very low concentrations both for macromolecular polymers and for supramolecular polymers. For macromolecular polymer adsorption n levels off abruptly and enters a pseudoplateau region, which is the regime that is almost exclusively found experimentally. In the case of supramolecular polymer adsorption beyond the Henry regime, n increases rapidly, and a pseudo-plateau-region is hardly observed in this case. So there is positive cooperativity for supramolecular polymers, but not for macromolecular polymers.

The partition functions of the supramolecular polymer systems were calculated on the quasi-chemical level of approximation. The partition functions of the macromolecular polymer systems, on the other hand, were obtained by means of the Scheutjens-Fleer theory, which includes excluded volume interactions on the Flory level only. However, the fact that this is a slightly different level of approximation is not relevant at all for the trends presented in this chapter. For example, the entropic factors in the equations that describe the shift of the adsorption isotherms cancel, because all nonlocal entropic factors are contained in the factors $f_0(N, \theta)$ and $f_0(\theta)$ in Eqs. (3.3) and (3.4). The magnitude of the shifts upon a variation in u_{LL} or χ_s is therefore completely independent of whether quasi-chemical or Scheutjens-Fleer calculations were used. Admittedly, there will be small effects on the shape of the isotherms and hence on the data presented in figures of Sec. 3.5. In any case using exactly the same level of approximation would lead to the same conclusions.

Like macromolecular polymers, supramolecular polymers can alter the properties of surfaces and they can switch between flat, hard layers and fluffy, soft adsorbed layers depending on experimental conditions. Unlike macromolecular polymers, however, supramolecular polymers can adsorb and desorb within a experimentally accessible concentration range. Adsorbed supramolecular polymers are therefore more responsive to changes in the monomer concentration. We expect that the results in this chapter will therefore increase the appreciation of supramolecular polymers as surface-modifying agents.

References

[1] M. E. Cates and S. J. Candau, J. Phys.: Condens. Matter **2**, 6869 (1990).
[2] F. Lequeux, Curr. Opin. Coll. Int. **1**, 341 (1996).
[3] R. S. Scott, J. Phys. Chem. **69**, 261 (1965).
[4] G. Faivre and J.-L. Gardissat, Macromolecules **19**, 1988 (1986).
[5] F. Oosawa and S. Asakura, *Thermodynamics of the Polymerization of Protein*, Academic Press, London, 1975.
[6] L. Brunsveld, B. J. B. Folmer, E. W. Meijer, and R. P. Sijbesma, Chem. Rev. **101**, 4071 (2001).
[7] R. Sijbesma et al., Science **278**, 1601 (1997).
[8] A. van de Craats et al., Adv. Mat. **11**, 1469 (1999).
[9] T. Vermonden et al., Macromolecules **36**, 7035 (2003).
[10] A. Ciferri, *Supramolecular Polymers*, Marcel Dekker, New York, 2000.
[11] D. H. Napper, *Polymeric Stabilization of Colloidal Dispersions*, Academic Press, London, 1983.
[12] E. Currie, W. Norde, and M. A. Cohen Stuart, Adv. Coll. Int. Sci. **100-102**, 205 (2003).
[13] V. Schmitt, F. Lequeux, and C. M. Marques, J. Phys. II France **3**, 891 (1993).
[14] Y. Rouault and A. Milchev, Macromol. Theory Simul. **6**, 1177 (1997).
[15] A. Milchev, Eur. Phys. J. E **8**, 531 (2002).
[16] J. van der Gucht and N. A. M. Besseling, Phys. Rev. E **65**, 051801 (2002).
[17] J. van der Gucht and N. A. M. Besseling, J. Phys. Condens. Matter **15**, 6627 (2003).
[18] J. van der Gucht, N. A. M. Besseling, and M. A. Cohen Stuart, J. Am. Chem. Soc. **124**, 6202 (2002).
[19] J. van der Gucht, N. A. M. Besseling, and G. J. Fleer, J. Chem. Phys. **119**, 8175 (2003).
[20] J. van der Gucht, N. A. M. Besseling, and G. J. Fleer, Macromolecules **37(8)**, 3026 (2004).
[21] A. Milchev and D. P. Landau, J. Chem. Phys. **104**, 9161 (1996).
[22] A. Hariharan, S. K. Kumar, and T. P. Russell, Macromolecules **23**, 3584 (1990).
[23] S. P. F. M. Roefs, J. M. H. M. Scheutjens, and F. A. M. Leermakers, Macromolecules **27**, 4810 (1994).
[24] H. J. A. Zweistra and N. A. M. Besseling, Phys. Rev. Lett. **96(7)**, 078301 (2006).
[25] G. J. Fleer, M. A. Cohen Stuart, J. M. H. M. Scheutjens, T. Cosgrove, and B. Vincent, *Polymers at Interfaces*, Chapman and Hall, London, 1993.
[26] J. P. Straley, J. Chem. Phys. **57**, 3694 (1972).
[27] C. M. Wijmans, F. A. M. Leermakers, and G. J. Fleer, J. Chem. Phys. **101**, 8214 (1994).
[28] C. C. van der Linden, F. A. M. Leermakers, and G. J. Fleer, Macromolecules **29**, 1172 (1996).
[29] N. A. M. Besseling and J. M. H. M. Scheutjens, J. Phys. Chem. **98**, 11597 (1994).
[30] R. Dickman and C. K. Hall, J. Chem. Phys. **85**, 3023 (1986).
[31] J. M. H. M. Scheutjens and G. Fleer, J. Phys. Chem. **83**, 1619 (1979).
[32] J. M. H. M. Scheutjens and G. Fleer, J. Phys. Chem. **84**, 178 (1980).
[33] J. M. H. M. Scheutjens and G. Fleer, Adv. Coll. Int. Sci. **16**, 361 (1982).
[34] G. J. Fleer, J. van Male, and A. Johner, Macromolecules **32** (1999).
[35] T. M. Birshtein, E. B. Zhulina, and A. M. Skvortsov, Biopolymers **18**, 1171 (1979).
[36] A. V. Hill, J. Physiol. (London) **40**, 4 (1910).

Chapter 4

Direct Determination of Liquid Phase Coexistence by Monte Carlo Simulations*

Abstract

A formalism to determine coexistence points by means of Monte Carlo simulations is presented. The general idea of the method is to perform a simulation simultaneously in several unconnected boxes which can exchange particles. At equilibrium, most of the boxes will be occupied by a homogeneous phase. The compositions of these boxes yield coexisting points on the binodal. However, since the overall composition is fixed, at least one of the boxes will contain an interface. We show that this does not affect the results, provided that the interface has no net curvature. We coin the name "Helmholtz-ensemble method," because the method is related to the well-known Gibbs-ensemble method, but the volume of the boxes is constant. Since the box volumes are constant, we expect that the method will be particularly useful for lattice models. The accuracy of the Helmholtz-ensemble method is benchmarked against known coexistence curves of the three-dimensional Ising model with excellent results.

4.1. Introduction

Phase coexistence of fluids is an important subject from both a scientific and a technological viewpoint. For example, the complex phase behavior of oil, water, and surfactants is interesting in its own right. Phase separation is also an important purification mechanism in the process industry.

Since the advent of the Metropolis algorithm[1] in the 1950s, Monte Carlo methods have been used extensively to simulate equilibrium properties of fluids. The Metropolis technique lets us sample a representative part of configuration space, which enables us to calculate thermodynamic properties of the system.

An important goal of simulations of immiscible fluids is to find the compositions of the coexisting phases. To this end, Panagiotopoulos introduced the so-called Gibbs ensemble method almost 20 years ago.[2] In his elegant scheme, the entire system is partitioned into two simulation boxes which can exchange both particles and volume.[2, 3] This method depends on the property that the systems tend to avoid the formation of an interface. After equilibration, no interface is found in either box. When the overall composition is in the two-phase regime, each box assumes the same composition as one

*Published as: H. J. A. Zweistra and N. A. M. Besseling, Phys. Rev. E **74**, 016111, (2006).

of the coexisting homogeneous phases. The results agree well with compositions that were calculated by earlier methods.

Elegant as this scheme may be, the Gibbs ensemble technique breaks down when one of the phases becomes very dense, since then the exchange of monomers between the systems becomes a highly unlikely event.[4] Lattice models of monomeric species do not suffer from this drawback. Lattice models have been in use for a long time in statistical mechanics. They usually require less computational time and memory than their continuum counterparts, and structural analysis of such systems is usually much simpler. Paradoxically, the determination of phase coexistence points has proved to be more involved with lattice models than with continuous-space models.

For instance, the Gibbs ensemble method can be applied to lattice models only with great difficulty. The principal problem that one has to solve is incorporating volume changes. In order to maintain periodic boundary conditions, only entire lattice layers can be transfered from one system to another. The probability that such an event occurs is very low due to the large number of contacts. Moreover, as the volumes can only be changed in relatively large discrete steps, the equilibrium volume ratio between the coexisting phases cannot generally be reached. The convergence speed is further deteriorated if polymers are present. However, Mackie *et al.* devised a scheme to improve the convergence behavior.[5, 6]

Indirect methods to determine phase coexistence points are more often used for lattice systems at the moment. Indirect methods, in contrast with direct methods, generally make use of a single simulation box. It is usually not possible to sample the concentrated and dilute phase directly from a single box because it is difficult to locate the phase boundaries. This is especially true near the critical point.

Instead, the free energy per unit volume of the system is calculated for a range of overall compositions. The coexistence points can then be calculated by means of a Maxwell construction (or variant thereof). Several authors reported quantitative results for coexistence curves calculated using the indirect determination. The development of the indirect method applied to water-oil-amphiphile systems is due to Larson *et al.*[7] Their method has been modified recently to study amphiphile solubility and phase behavior in supercritical CO_2.[8, 9] Yan *et al.* used an indirect method to obtain an accurate coexistence curve for the three-dimensional Ising lattice, which is equivalent to a binary mixture with symmetric interaction potentials.[10]

However, the problems associated with the indirect method are twofold. First, by comparison elaborate calculations are required in order to obtain accurate results, since the initial composition has to be varied over a broad range in order to obtain a single point on the coexistence curve. Second, in practice only systems that separate into two phases can be modeled. It is in principle possible to simulate phase behavior of a multi-phase system, but this involves the calculation of a multidimensional Maxwell

construction. The computational cost of such a calculation is astronomical as the concentration of each component would have to be varied independently.

Finally, we mention the Kofke method to trace the coexistence curve.[11–13] This method cannot be categorized as a direct or indirect method to calculate phase coexistence points. Rather, it depends on *a priori* methods to find a single point on the binodal. The other points are then found by integrating the Clausius-Clapeyron equation along the coexistence line. This method proved to be useful and it is extensively used. In its original form, it may be unstable[4] and numerical errors make that the result tends to grow away from the "true" coexistence line. Mehta and Kofke proposed a modification of the algorithm[14] that circumvents the numerical instability. Their modification works especially well for compositions that are not too close to the critical point. At any rate, this method still depends on *a priori* methods so the demand for fast and accurate direct and indirect methods will not diminish because of the development of the Kofke integration.

In this chapter, we introduce a direct method to determine phase coexistence points by means of Monte Carlo simulations. This chapter is organized as follows. In Sec. 4.2, we will describe the method in general terms and provide justification for our method based on thermodynamic arguments. In Sec. 4.3, we will benchmark the accuracy of the method against known results for the 3D Ising lattice.

4.2. Description of the method

The general idea of the method is to simulate phase coexistence in several unconnected boxes which can exchange particles. Most of the boxes will contain a homogeneous phase. The composition of those boxes is used to determine the phase coexistence points. In contrast with the Gibbs-ensemble, volume changes are not needed, but we deliberately allow an interface to be formed in one of the boxes instead. Boxes that contain an interface are not used for the determination of coexistence points.

If monomeric, isotropic particles are involved, only one type of perturbation is needed: particle displacements. This is necessary and sufficient to reach the phase-separated state from any random configuration. If more complex particles are involved, also particle rotations, reorientations and possibly reconfigurations should be implemented. These perturbations are not specific for this method but have to be employed in any correct Monte Carlo sampling. We will restrict the discussion to monomeric, isotropic species, but without loss of generality. The principle of the method is not altered in any way if more elaborate perturbations of the particles have to be included in the Monte Carlo scheme.

The formalism can be justified on thermodynamic grounds. Consider a macroscopic, phase-separated system containing P coexisting phases, which are connected by I surfaces. At thermodynamic equilibrium, the chemical potential of any component and the pressure are constant throughout the system.

We are free to arbitrarily partition the macroscopic system into several unconnected simulation boxes which can exchange particles. Particle displacement is sufficient to induce phase separation in a macroscopic mixture. Hence phase separation will also occur in a collection of particle-interchanging boxes. However, this does not happen for each box individually, but rather for the ensemble of boxes as a whole. It is unlikely that a homogeneous phase will develop an interface because an interface contributes to the free energy of the system.[4]

The important consequence of this is that as many boxes as possible will contain a homogeneous phase. One or several boxes will have to contain an interface, because the overall composition is conserved. The number of interface-containing boxes will not exceed I, the number of interfaces that were present in the macroscopic system, because the interface area is minimal at thermodynamic equilibrium. We conclude that we can find the compositions of the coexisting phases directly if we perform the simulation in at least $P+I$ particle-interchanging boxes simultaneously. After equilibration, we identify boxes that contain a homogeneous phase as coexisting phases in the macroscopic system.

Note that the computational demands of this method scale much more favorably with the number of coexisting phases than indirect methods. In the present method, only a few boxes need to be added in a single computer experiment, while in the case of indirect methods, another *dimension* should be added to the Maxwell construction for each additional phase. However, we will restrict the discussion in this article to two-phase systems.

Several features of the present method will be illustrated by means of an example: simulating phase coexistence of a binary liquid mixture. We will use lowercase letters a and b to refer to the components in the mixture. The composition of the system is determined by the overall volume fractions of the components: ϕ_a and ϕ_b.

The components a and b are only partially miscible, therefore the mixture will segregate into an a-rich and a b-rich phase. These phases are named here simply A and B, respectively. We are interested in the compositions of the coexisting phases: ϕ_a^A (the volume fraction of component a in phase A), ϕ_b^B (the volume fraction of component b in phase B), and so on.

Two phases and one interface exist, so we will use three simulation boxes and enforce full periodic boundary conditions. This is schematically depicted in Fig. 4.1. The system is initialized by filling the boxes at random for a given initial composition. During equilibration, particles are exchanged between boxes I, II and III (indicated by

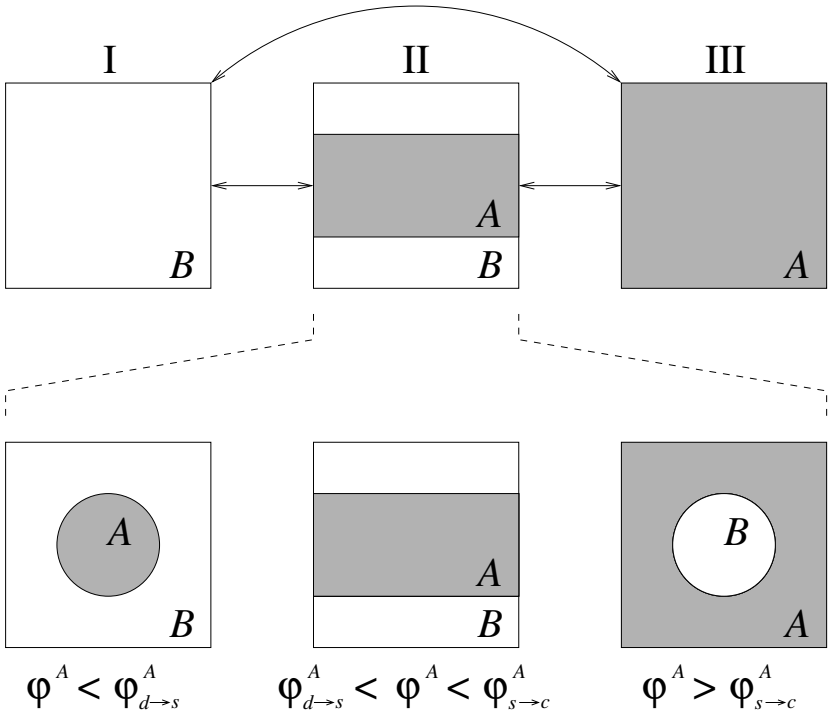

Figure 4.1. Schematic illustration of the proposed method for a binary mixture. See text for details.

bidirectional arrows). Particles can also be displaced within a single box. The boxes are therefore in thermodynamic equilibrium internally and with the other boxes.

It is usually not possible to predict which boxes will develop a homogeneous phase from the random configuration of particles. In this specific simulation, boxes I and III contain homogeneous phases B and A after equilibration. Therefore we use the composition of boxes I and III to find the coexistence points: $\phi_a^B = \phi_a^I$, $\phi_b^B = \phi_b^I$, $\phi_a^A = \phi_a^{III}$, and $\phi_b^A = \phi_b^{III}$.

Box II *must* contain an interface because the total composition is conserved. The initial (or overall) composition of the boxes determines the composition of box II, and thus the volume that is occupied by phase A in II. The *phase volume fraction* of phase A in box II is indicated by φ^A. The shape of phase A in box II is determined by φ^A since the shape of the phase is adjusted in order to minimize the surface area (Fig. 4.1).

At low φ^A, phase A forms a droplet (d) inside a continuous phase B (Fig. 4.1). If φ^A is increased above a certain droplet-to-slab transition volume fraction $\varphi^A_{d\to s}$, the formation of a "slab" of phase A becomes favorable since it has a smaller surface area than a droplet of the same volume. The system passes a second transition $\varphi^A_{s\to c}$ at even higher values of φ^A. The situation is now reversed: phase A forms a continuous phase (c) around phase B.

The shape of phase A in box II is of relevance because a pressure difference, known as the Laplace pressure, exists across a curved interface.[15] The Laplace pressure influences

the chemical potentials of the box containing the interface, and also the chemical potentials of the collection of boxes as a whole. The composition of the homogeneous boxes is therefore affected by a nonzero average curvature of the interface. Box II should contain an interface with vanishing average curvature in order to obtain accurate results. Note that an interface with vanishing average curvature is formed when $\varphi^A_{d\to s} < \varphi^A < \varphi^A_{s\to c}$.

It is therefore of interest to estimate $\varphi^A_{d\to s}$ and $\varphi^A_{s\to c}$. For the moment, we will assume that: (i) surface roughness does not contribute to the total surface area in a significant way, and (ii) the composition of the different phases on both sides of the interface does not depend on the average curvature of the interface. Surface free energy is then the only quantity that needs to be minimized. For a given φ^A, phase A adjusts its shape to minimize the surface free energy. The value of $\varphi^A_{d\to s}$ then follows from simple geometric considerations, since it is the value of φ^A where the surface area of a droplet equals the surface area of a slab. The value of $\varphi^A_{s\to c}$ follows from equivalent arguments, and we obtain

$$\varphi^A_{d\to s} = \frac{1}{3}\sqrt{\frac{2}{\pi}} \approx 0.266, \tag{4.1}$$

$$\varphi^A_{s\to c} = 1 - \frac{1}{3}\sqrt{\frac{2}{\pi}} \approx 0.734. \tag{4.2}$$

To a first approximation, we expect to find an on average flat interface if the phase volume fractions of the box containing the interface lie roughly in between these values.

The approximations used in this argument may prove to be quite severe. Larson *et al.* observed that the interface of a segregated system with symmetric interactions can exhibit a large degree of surface roughness.[7] Moreover, $\phi_a^{II,A}$ and $\phi_a^{II,B}$ are not completely independent of the curvature of the surface. Nonetheless, it gives some idea of how the system reacts to a mismatched phase volume fraction.

Direct assessment of φ^A is not straightforward, as it requires the determination of a dividing plane between the two phases. It is much more convenient to measure ϕ_a^{II}, the volume fraction of component a in system II, instead. In certain special cases, it is possible to check that $\varphi^A \approx 0.5$, which is desirable in any situation. For example, when the phases are strongly segregated, $\phi_a^{II,A} \approx 1 \gg \phi_a^{II,B}$ therefore φ^A and ϕ_a^{II} are roughly equal in this case. Furthermore, if interactions between the particles are symmetric, the volume fractions of the phases must be equal if the volume fractions of the particles are equal, which is easy to check.

If one is interested in a complex model at high temperatures, no direct relation between φ^A and ϕ_a^{II} is known. In such a case, one should check if a simulation with a slightly different initial composition leads to the same composition of the homogeneous phases. Alternatively, one could use for instance Widom's test-particle method[16] to determine the chemical potentials of the equilibrated system, and check if they do not

depend on ϕ_a. If this is the case, it can be assumed that the interface is on average flat and that the chemical potential (and thus the compositions) are correct.

In the case that a curved interface is formed, one can simply adjust the overall composition and redo the simulation. It is therefore in principle always possible to find the compositions of two coexisting phases, even if the interaction potentials are highly asymmetric. The range of applicability is therefore not affected by the possible occurrence of a curved interface.

It would be worthwhile for future research to find expressions to improve the estimation of φ^A and the average curvature of the interface from ϕ_a^{II}. Such an analysis should at least take the surface tension and roughness and the size of the droplet into account. If these expressions are available, it is possible to define explicit criteria which the composition of the interface box must satisfy in order to have a interface without net curvature.

If the interface has no average curvature, we can use the compositions of the boxes that contain homogeneous phase to obtain a direct determination of the phase coexistence points. In contrast to the original Gibbs-ensemble method,[2] volume exchanges are unnecessary in this scheme. This methodology is therefore both easier to implement and much more suitable for lattice systems.

We propose the term "Helmholtz-ensemble method" for our method for several reasons. First, equilibration of the boxes is equivalent to minimization of the Helmholtz energy. The collection of boxes comprises a system within the canonical ensemble. Equilibrium is reached when the Helmholtz free energy of such a system is minimal.[15] Moreover, we would like to indicate the connection with the Gibbs-ensemble method. The most important difference between the present method and the Gibbs-ensemble method is that the volumes of the boxes are constant in the present method, while it is variable in the Gibbs-ensemble method. The fact that the simulations are performed at constant volume also explains our choice for the term Helmholtz-ensemble method.

Gibbs-ensemble and Helmholtz-ensemble calculations both yield coexistence points at constant pressure. The pressures are the same in each box, as this is one of the conditions of phase coexistence at thermodynamic equilibrium. This is in contrast with the method by Nelson *et al.*[17] This method is based on performing a simulation in two boxes simultaneously. Particle exchanges between the boxes are allowed for all but one of the particle types. This method has been used to calculate partition coefficients of oil in water in the presence and absence of amphiphiles.

Although similar to the present method in the sense that the box volumes are constant and that only particle displacements are necessary to reach equilibrium, there are fundamental differences. In Nelson *et al.*'s method, an osmotic pressure difference arises between the boxes, because particle exchange between the boxes is disallowed for

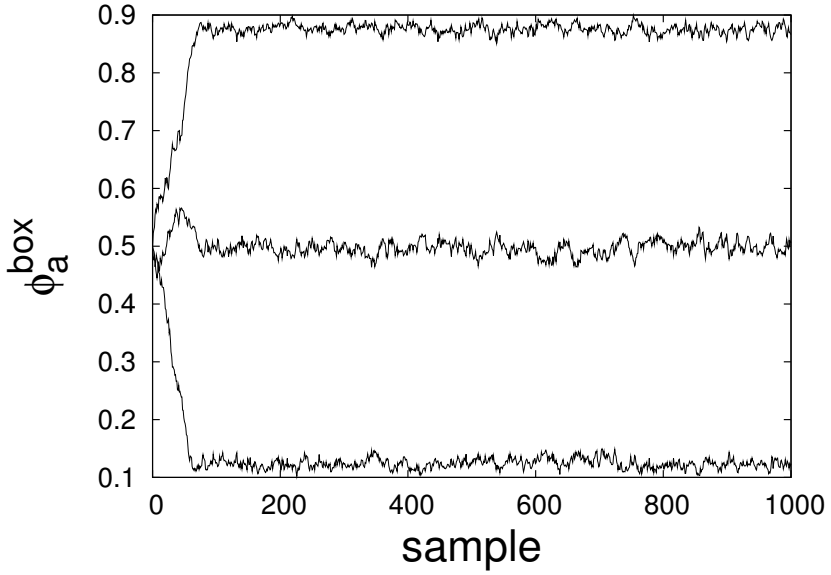

FIGURE 4.2. Sample run for the 3D Ising model at $T^* = 1.0$. The volume fraction of component a is plotted against the sample ranking number for each box individually. Between samples, 10^5 swaps were attempted.

one of the species. Nelson *et al.*'s method is therefore not suitable to calculate phase coexistence points at arbitrary compositions.

4.3. Numerical results for the 3D Ising model

In this section, we will present results that validate our method. Up to this point, we did not make a distinction between continuous and lattice systems. The Helmholtz-ensemble method is equally applicable to both types of systems. We will discuss only lattice models in this section, because it is to expected that the Helmholtz ensemble is superior to the Gibbs-ensemble method for lattice systems.

We chose the 3D Ising lattice to benchmark the method. The 3D Ising lattice is equivalent to phase separation of a binary mixture with symmetric interaction potentials. The Ising model is a convenient choice because the properties of this model are reasonably well known. Moreover, the model is symmetric with respect to the exchange of two species. As a result, the interface is guaranteed to be on average flat if $\phi_a = \phi_b = \frac{1}{2}$. The Helmholtz ensemble is equally applicable to systems with asymmetric interactions. If we apply the Helmholtz-ensemble method to such a model, we have to explicitly check that the interface is on average flat. The overall composition should be adjusted accordingly if this is not the case.

In the 3D Ising lattice, space is discretized into cubic lattice sites, and only nearest neighbor interactions are taken into account. Boxes of $20 \times 20 \times 20$ lattice sites and

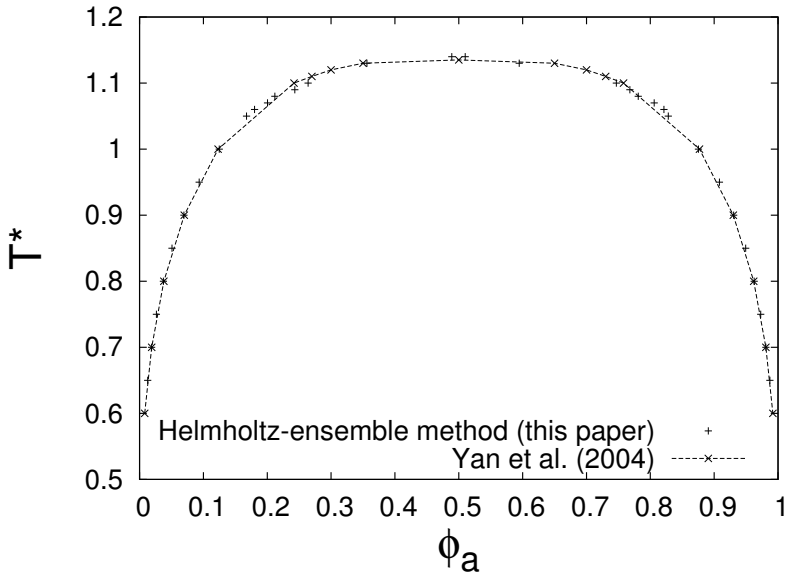

Figure 4.3. Coexistence curves calculated by means of the Helmholtz-ensemble method benchmarked against accurate results by Yan *et al.*[10] Used with permission from the authors.

periodic boundary conditions were used. Each box had the same initial composition and the initial configuration of each box was random.

Only random particle exchanges were used to reach equilibrium. An internal energy change ΔE was calculated for each perturbation. The change was accepted when $\Delta E \leq 0$ or with probability $\exp(-\beta\Delta E)$ when $\Delta E > 0$, where $\beta = (kT)^{-1}$, T the temperature and k is Boltzmann's constant. This is simply the Metropolis scheme to traverse phase space.[1] Pseudorandom numbers were generated using the Mersenne twister algorithm[18] which has a very large period and a uniform distribution.

Interactions between unlike particles are described by the parameter ϵ:

$$\epsilon = 2\epsilon_{12} - \epsilon_{11} - \epsilon_{22}, \tag{4.3}$$

in which the $\epsilon_{\alpha\beta}$ represents the energy of a contact between a particle of type α and a particle of type β. The reduced temperature of the Ising system is defined as

$$T^* = \frac{kT}{\epsilon}. \tag{4.4}$$

The parameter ϕ_a was 0.50 to ensure that the interface is flat on average after equilibration. A sample run is shown in Fig. 4.2. The entire coexistence curve, together with the accurate Monte Carlo results of Yan *et al.* from Ref.,[10] is depicted in Fig. 4.3. The two plots coincide over the entire concentration range. Our method works surprisingly well near the critical point and the results are indistinguishable from Yan *et al.*'s Monte Carlo data at lower T^*.

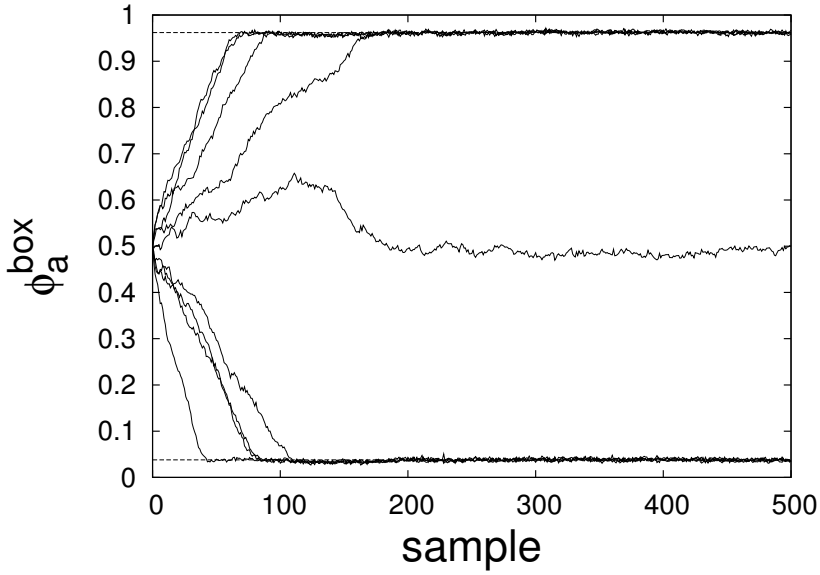

Figure 4.4. Evolutions of volume fractions of component a in the 3D Ising system at $T^* = 0.8$ for a run containing nine boxes. The volume fraction of component a in the boxes is plotted against the sample ranking number for each box individually. Between samples, 5×10^5 particle swaps were attempted. The compositions published in Ref.[10] are shown with a dashed line.

A rerun of the Ising lattice at $T^* = 0.8$, but now for nine boxes, yielded eight homogeneous boxes and only one box containing an interface (Fig. 4.4). This clearly corroborates our prediction that as many boxes as possible will develop a homogeneous phase due to the free energy contribution of an interface.

The effect of ϕ_a on the equilibrium composition of the homogeneous phases is shown in Fig. 4.5. Apparently, ϕ_a^B depends significantly on the initial composition. This plot exhibits a clear plateau at the correct composition around $\phi_a = 0.5$, which is the region where we expect to find a surface with vanishing average curvature. Significant errors are found outside that plateau region, which is most likely due to the formation of a curved interface. The errors continue to grow if we move away from the plateau, since the further away from the plateau, the smaller the phase droplets are, and the Laplace pressure scales with the inverse radius of the droplet.

The results shown in Fig. 4.5 indicate that the regime of flat interfaces is narrower than predicted by our first order estimation. Still, it shows that a substantial volume fraction regime exists where very accurate results can be obtained. Finally, it is noted that the possibility of the formation of a curved interface does not limit the applicability of the Helmholtz-ensemble method. If it is found that the interface has a finite average curvature, then the overall composition should be adjusted accordingly and the simulation should be repeated. The Helmholtz-ensemble method is therefore capable of

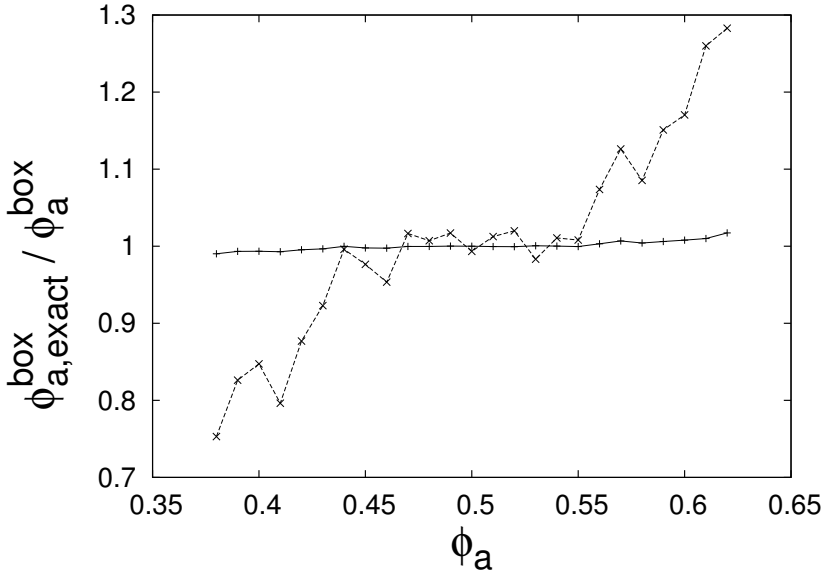

FIGURE 4.5. 3D Ising model at $T^* = 0.8$. This plot shows the accuracy of the Helmholtz-ensemble method relative to the "exact" volume fractions from Yan *et al.*[10] The superscript "box" refers to the homogeneous box which was used to determine the compositions of phases A and B. The ratios $\phi^A_{a,exact}/\phi^A_a$ (solid line) and $\phi^B_{a,exact}/\phi^B_a$ phases (dotted line) are plotted against the initial volume fraction ϕ_a. Note the plateau region where $\phi^B_{a,exact}/\phi^B_a = 1$; this indicates the region where an on average flat interface is present.

calculating phase coexistence for systems with symmetric interactions and for systems with asymmetric interactions.

4.4. Conclusions and recommendations

In this chapter, we introduce the Helmholtz-ensemble method: a formalism to determine the composition of coexisting phases by a single Monte Carlo experiment. In contrast with the Gibbs-ensemble method by Panagiotopoulos, volume changes are unnecessary. The present method is therefore especially useful for lattice models. Moreover, the Helmholtz-ensemble method method is both faster and more flexible than current methods for lattice systems, which are usually based on free energy calculations.

The phase coexistence points for a 3D Ising model that were obtained with the Helmholtz-ensemble method are in very close agreement with accurate results from existing literature. Although we benchmarked the method against a simple lattice model system involving monomeric, isotropic particles, the work presented here is easily extended to continuous and/or more complex models. We therefore expect that the method presented here will be very useful to elucidate the phase behavior of, for instance, polymers and surfactants.

References

[1] N. Metropolis, A. W. Rosenbluth, M. N. Rosenbluth, A. H. Teller, and E. Teller, J. Chem. Phys. **21**, 1087 (1953).
[2] A. Z. Panagiotopoulos, Mol. Phys. **61**, 813 (1987).
[3] A. Z. Panagiotopoulos, Mol. Sim. **9**, 1 (1992).
[4] D. Frenkel and B. Smit, *Understanding Molecular Simulation*, Academic Press, London, 2002.
[5] A. D. Mackie, A. Z. Panagiotopoulos, D. Frenkel, and S. K. Kumar, Europhys. Lett. **27**, 549 (1994).
[6] A. D. Mackie, A. Z. Panagiotopoulos, and S. K. Kumar, J. Chem. Phys. **102**, 1014 (1995).
[7] R. G. Larson, L. Scriven, and H. T. Davis, J. Chem. Phys. **83**, 2411 (1985).
[8] M. Lísal, C. K. Hall, K. E. Gubbins, and A. Panagiotopoulos, J. Chem. Phys. **116**, 1171 (2002).
[9] L. F. Scanu, K. E. Gubbins, and C. K. Hall, Langmuir **20**, 514 (2004).
[10] Q. Yan, H. Liu, and Y. Hu, Fluid Phase Equil. **218**, 157 (2004).
[11] D. A. Kofke, Mol. Phys. **78**, 1331 (1993).
[12] D. A. Kofke, J. Chem. Phys. **98**, 4149 (1993).
[13] D. A. Kofke, Adv. Chem. Phys. **105**, 405 (1999).
[14] M. Mehta and D. A. Kofke, Chem. Eng. Sci. **49**, 2633 (1994).
[15] P. Atkins and J. de Paula, *Physical Chemistry*, Oxford University Press, Oxford, 7th edition, 2002.
[16] B. Widom, J. Chem. Phys. **39**, 2802 (1963).
[17] P. H. Nelson, T. A. Hatton, and G. C. Rutledge, J. Chem. Phys. **110**, 9673 (1999).
[18] M. Matsumoto and T. Nishimura, Trans. Mod. Comp. Sim. **8**, 3 (1998).

Chapter 5

Monte Carlo Study of Supramolecular Polymer Fractionation: Selective Removal of Chain Stoppers by Phase Separation*

Abstract

Supramolecular polymers consist of bifunctional monomers that join and break reversibly. Supramolecular polymer solutions are often polluted by monofunctional contaminants, which drastically reduces the chain-forming capabilities of the system. Unfortunately, the monofunctional contaminants are difficult to remove due to the physical and chemical resemblance with the bifunctional counterparts. In this chapter, we present a method to specifically remove the monofunctional contaminants from a supramolecular polymer solution. The general idea is to induce phase separation by decreasing the solvent quality, and to remove the most dilute phase. This concept is explored by means of a recently developed Monte Carlo scheme to calculate the compositions of the coexisting liquid phases. The simulations provide a proof of principle that the proposed purification method is suitable to remove the monofunctional contaminants efficiently. The calculations indicate that, at the right experimental conditions, the vast majority of the monofunctional contaminants can be removed in this way while most of the bifunctional monomers are retained. Because of the general nature of the arguments presented here, it is to be expected that the results are applicable to a large variety of supramolecular systems. Moreover, the method is very suitable for large-scale applications because only solvent is added and no tedious chromatographic steps are required.

5.1. Introduction

Supramolecular polymers are linear aggregates which consist of monomers that are joined by reversible bonds. The *functionality* of a monomer is equal to the number of bonding groups of a monomer. To achieve the formation of linear chains, the monomers should be bifunctional. Many of such compounds have been synthesized in recent years. Synthetic monomers usually consist of two binding groups that are connected by a spacer.[1] They can be categorized according to the nature of the reversible bond between the monomers:[1, 2] hydrogen-bonded,[3–5] discotic,[6] and coordination[7] supramolecular polymers. Monofunctional monomers often occur as an unwanted by-product in

*Published as: H. J. A. Zweistra,N. A. M. Besseling, and M. A. Cohen Stuart J. Phys. Chem. B **110(37)**, 18629-18634, (2006).

the synthesis of bifunctional monomers.[1, 3, 8] They are detrimental to the effectivity of the supramolecular polymer system because monofunctional monomers form additional chain ends and hence reduce the average degree of polymerization. They are therefore sometimes called 'chain stoppers'. Controlling the amount of chain stoppers is essential to control the properties of the supramolecular polymers. It is usually very difficult to remove the monofunctional contaminants, because of the large degree of chemical and physical similarity with their bifunctional counterparts.

We propose a new method to remove monofunctional contaminants from supramolecular polymer solutions. The general idea is to induce phase separation by decreasing the solvent quality and to subsequently discard the phase that is poor in polymer. The average chain length increases with concentration,[9] hence it is to be expected that the number of chain ends per monomer is larger in the dilute phase than in the concentrated phase. Because the monofunctional monomers are always at a chain end, it is to be expected that the dilute phase is enriched in monofunctional monomers. The supramolecular polymer solution can therefore be purified by inducing phase separation and to subsequently discard the dilute phase.

Phase separation methods are frequently used to purify samples of synthetic covalent polymers. In such a procedure, a large amount of poor solvent is added to a polydisperse polymer solution which induces precipitation of the longest chains. This method is in general use to narrow down the size distribution of the polymers.[10] However, as far as we know, phase separation has not been used to specifically remove chain stoppers from supramolecular polymer solutions.

In this chapter, we will explore the proposed method by simulations of a simple molecular model. The simulation results therefore do not apply to a specific system, but serve as a 'proof of principle' for a broad range of experimental systems. This chapter is organized as follows. In the next Section (5.2), we will first describe our simulations of phase separated supramolecular polymer solutions. From these simulations, we can construct the entire phase diagram from which the efficacy and selectivity of the method are easily determined. Unfortunately, it is not possible to simulate the purification process directly for realistic parameters of experimental systems, therefore extrapolations are necessary, as described in Section 5.3. These extrapolations provide a good estimate of the effectivity of the purification process in many situations.

5.2. Monte Carlo simulations

5.2.1. Description of the model

The idea to remove monofunctional contaminants by means of phase separation will be explored by Monte Carlo simulations. These calculations yield in principle 'exact' results[11] and have been used extensively to simulate equilibrium properties of supramolecular polymers.[12–16] Moreover, in contrast with mean-field theories, the magnitude of

the error does not depend on the concentration. Since the advent of the Gibbs-ensemble method, simulations of coexisting liquids have been predominantly performed for continuum systems.[17] However, a lattice model is more appropriate in this case for two reasons. First, the functionality of the monomers can be implemented in a very straightforward manner in lattice systems. Second and most important, the simulation of lattice systems does not break down when one of the phases becomes very dense.[11] Until recently, simulating phase separation of lattice models proved to be quite cumbersome. Therefore, two of us developed a new method a short while ago. This method, called the 'Helmholtz ensemble', enables one to simulate phase separation in lattice systems efficiently by means of Monte Carlo simulations.[18]

The supramolecular polymer solution in the presence of monofunctional monomers is modeled as follows. The solution is partitioned into cubic lattice sites. Three molecular species are present: bifunctional monomers, monofunctional monomers, and solvent molecules. Each type of molecule occupies a single site in the lattice. The molecules have six 'faces' by which they make contact with their neighbors. We discriminate between several types of faces with different properties. For example, an energy penalty of $+0.5kT$ is assigned to each contact between a face on a monomer and a face on a solvent molecule. The solvent quality is therefore poor, and monomers and solvent molecules tend to phase separate spontaneously.

Furthermore, 'linking faces' determine the connectivity of monomers. A reversible bond is formed between two adjacent monomers if linking faces on each monomer are pointed toward each other. A 'bond energy' E is assigned to each reversible bond. The value of E has to be negative in order to obtain appreciable chain formation. The functionality of a monomer is in this model simply the number of linking faces that a monomer possesses: bifunctional monomers have two linking faces, while monofunctional monomers have only one (Fig. 5.1).

5.2.2. Simulation results

A simulation snapshot for $E = -6kT$ is shown in Fig. 5.2. From simulations at different compositions, the entire phase diagram was calculated (Fig. 5.3).

A straight line through the lower left corner of the phase diagram can be called a 'dilution line'. Compositions that belong to points along such a line differ only in the concentration of solvent molecules; the ratio of mono- and bifunctional monomers remains the same. Careful inspection of Fig. 5.3 reveals that the tielines are less steep than the dilution lines originating from any of the points on that tieline (except for the case $X_{mono} = 0$). This can be used to remove the monofunctional contaminants, as is graphically shown in Fig. 5.4. Because the entire phase diagram is known, we can simulate an arbitrary number of purification steps according to this scheme.

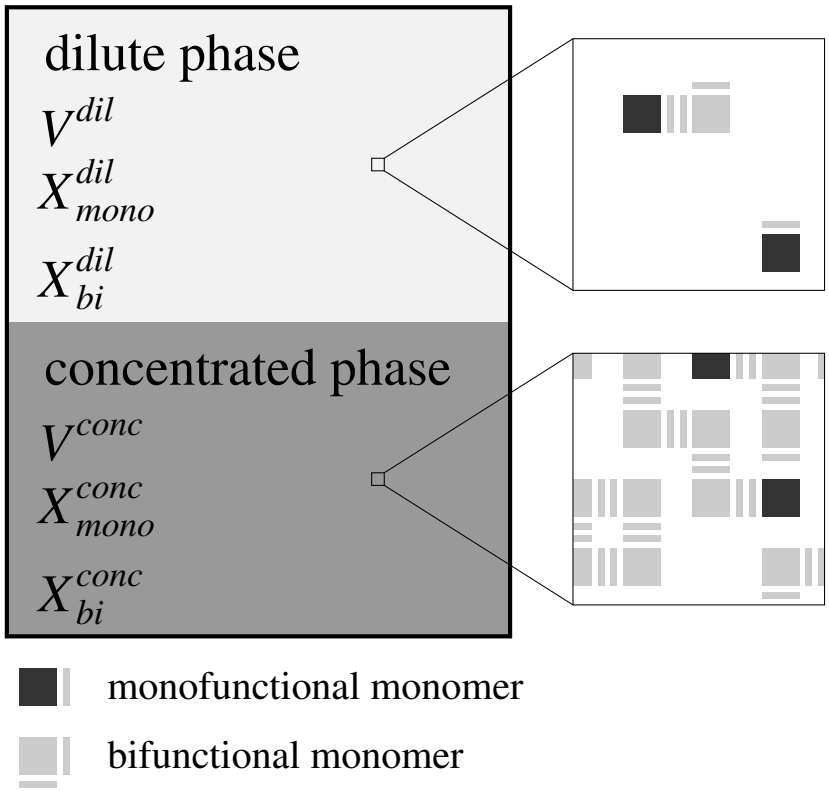

Figure 5.1. Schematic two-dimensional representation of the model system. An initially homogeneous supramolecular polymer solution is allowed to phase separate into a dilute and concentrated phase, each with a certain volume V, and mole fractions of mono- and bifunctional monomers X_{mono} and X_{bi}.

The efficacy of the purification process is characterized by both the degree of purification and the yield of bifunctional monomers. Hence we define the purification parameter $p = X_{mono}/X_{bi}$ at total polymer mole fraction $X^*_{pol} = X_{mono} + X_{bi}$ (Fig. 5.4). When the monofunctional contaminant concentration vanishes, $p \to 0$. Furthermore, the yield Y is defined as the fraction of the amount of bifunctional material that has been retained.

Figure 5.5 shows that p decreases with the number of purification steps n as expected. Some bifunctional monomer is inevitably discarded with the dilute phase, so the yield decreases with n as well. The volume of the dilute phase, and thus the amount of monomer that is discarded after each step, decreases with X^*_{pol}, so both p and the yield decrease faster with n when X^*_{pol} is small.

5.3. Analysis of the purification process

5.3.1. Parameterization of the phase diagram

While the results shown in Figs. 5.3 and 5.5 are accurate, they underestimate the efficacy of the purification method for typical real supramolecular systems. Because of

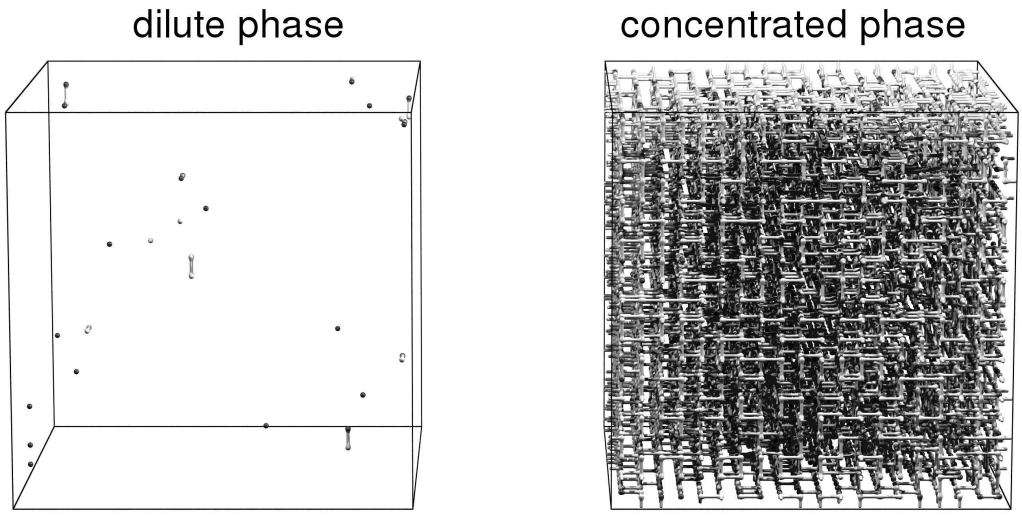

Figure 5.2. Snapshots of simulation boxes of the coexisting concentrated and dilute phases. Monofunctional monomers are drawn in dark grey, bifunctional monomers in light grey, and the solvent is not depicted for ease of viewing. The size of the simulation boxes is $20 \times 20 \times 20$ lattice sites and the bond energy is $-6kT$. Note that the relative occurrence of monofunctional monomers is greater in the dilute phase than in the concentrated phase.

technical limitations of the Monte Carlo simulation, the bond energy in our calculations of the phase diagram was $-4kT$. In reality, values in the range -10 to $-20kT$ are found, for example, in the case of triple and quadruple hydrogen-bonding supramolecular polymers.[1, 4, 19, 20] Because the chains are in reality longer than those in the Monte Carlo simulation, it is to be expected that the purification method will be more efficient in reality than as portrayed in Fig. 5.5.

The changes of p and Y with the number of purification steps, as depicted in Fig. 5.5, were based on extensive simulations. In the present section, it is shown that p and Y can be captured elegantly in a few simple explicit expressions. With the help of these, the number of required simulations is dramatically reduced. Moreover, systems with more negative bond energies, for which the simulations are computationally demanding, can be handled more easily.

The general idea is to characterize the phase diagram by three readily obtained parameters: C_0, D_0, and α. Parameters C_0 and D_0 are the bifunctional monomer concentrations of the coexisting phases in the absence of monofunctional contaminants (cf. Fig. 5.4). Furthermore, α is the ratio of the slopes of the tieline (DC) and the dilution line (SC). It was checked that α is insensitive to the position in the phase diagram: for the case of $E = -4kT$, the deviations in α were on the order of 0.2% when moving from $X^*_{pol} = X_{mono}$ to $X^*_{pol} = X_{bi}$. Therefore C_0, D_0, and α can be regarded as

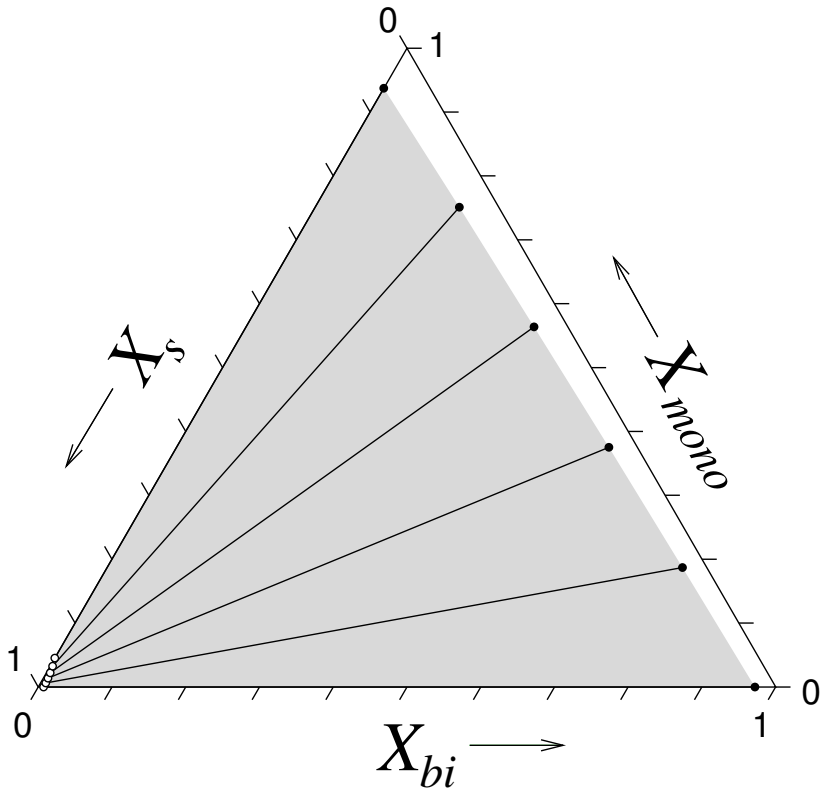

Figure 5.3. Phase diagram of a supramolecular polymer solution in the presence of monofunctional monomers. The bond energy is $-4kT$. The mole fractions of bifunctional monomers, monofunctional monomers and solvent molecules are represented by X_{bi}, X_{mono}, and X_s, respectively. All possible compositions correspond to a point in this diagram. The tielines connect a composition of the dilute phase (open circles) with a composition of the coexisting concentrated phase (filled circles). The region of compositions where phase separation occurs, is depicted in light grey. Any homogeneous phase with a composition inside the grey area is thermodynamically unstable and will phase separate into the dilute and concentrated phase that lie on the same tieline.

intrinsic properties of the phase diagram. In the present section, we demonstrate that these parameters, together with X^*_{pol} (which one can choose), are sufficient to predict the effectivity of the purification in the limit of low chain stopper concentrations.

Let us first define $R_p = p_n/p_{n-1}$, the ratio of the p-values of two consecutive purification steps. Similarly, $R_Y = Y_n/Y_{n-1}$ is defined.

To calculate R_p, we require p_n and p_{n-1}. From Fig. 5.4 it follows directly that $p_n = X^C_{mono}/X^C_{bi}$. On the other hand, p_{n-1}, which is equal to $X^{n-1}_{mono}/X^{n-1}_{bi}$, is calculated

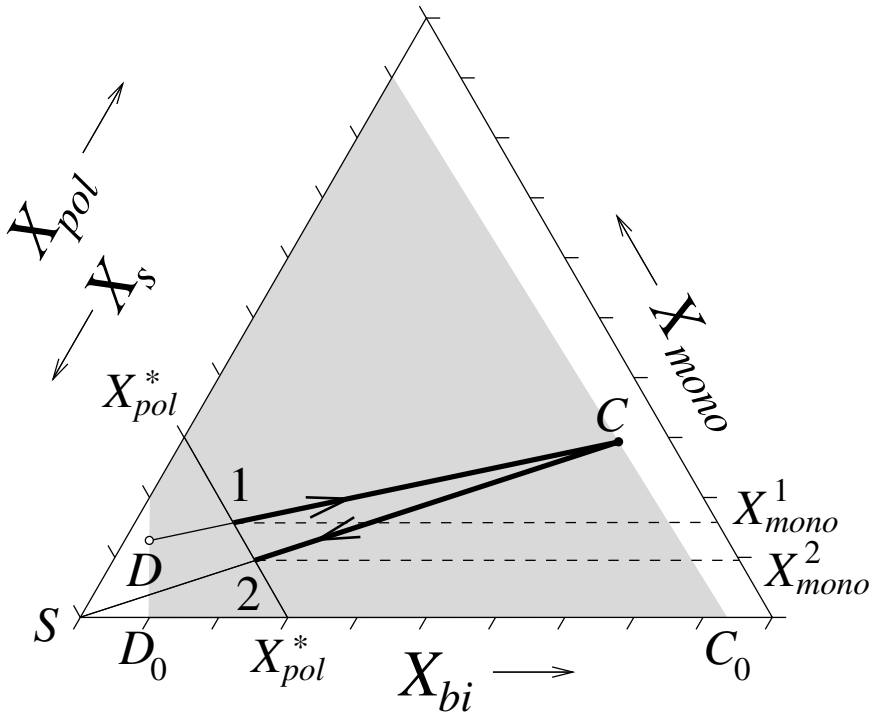

FIGURE 5.4. Cartoon of the purification method. The tieline shown in this figure is somewhat tilted for clarity. The total polymer content $X_{pol} = X_{bi} + X_{mono}$ is equal to $1 - X_s$, so the X_{pol} axis runs in the opposite direction from X_s. The purification is started in point 1 at a certain total polymer mole fraction X^*_{pol} and monofunctional monomer concentration X^1_{mono}. Point 1 lies within the phase separated region, and will therefore spontaneously separate into compositions C and D. The dilute phase is removed, and the concentrated phase is diluted with solvent along the SC line, until the total polymer concentration is again equal to X^*_{pol} (point 2). Note that $X^2_{mono} < X^1_{mono}$ because the dilution line SC is steeper than the tieline DC.

from the following set of equations:

$$\begin{cases} X^{n-1}_{mono} + X^{n-1}_{bi} = X^*_{pol} \\ \alpha \frac{X^C_{mono}}{X^C_{bi}} = \frac{X^C_{mono} - X^{n-1}_{mono}}{X^C_{bi} - X^{n-1}_{bi}} \end{cases}$$

After some manipulation, it is found that

$$R_p = \frac{\alpha X^C_{mono} - X^C_{mono} + X^*_{pol}}{X^C_{bi}\left(1 - \alpha + \frac{\alpha X^*_{pol}}{X^C_{bi}}\right)}. \tag{5.1}$$

The value of R_Y follows from the mass balance of the bifunctional monomers, and can be shown to be

$$R_Y = \frac{X^C_{bi}\left(X^*_{pol} - X^D_{bi}\right)}{X^*_{pol}\left(X^T_{bi} - X^D_{bi}\right)}. \tag{5.2}$$

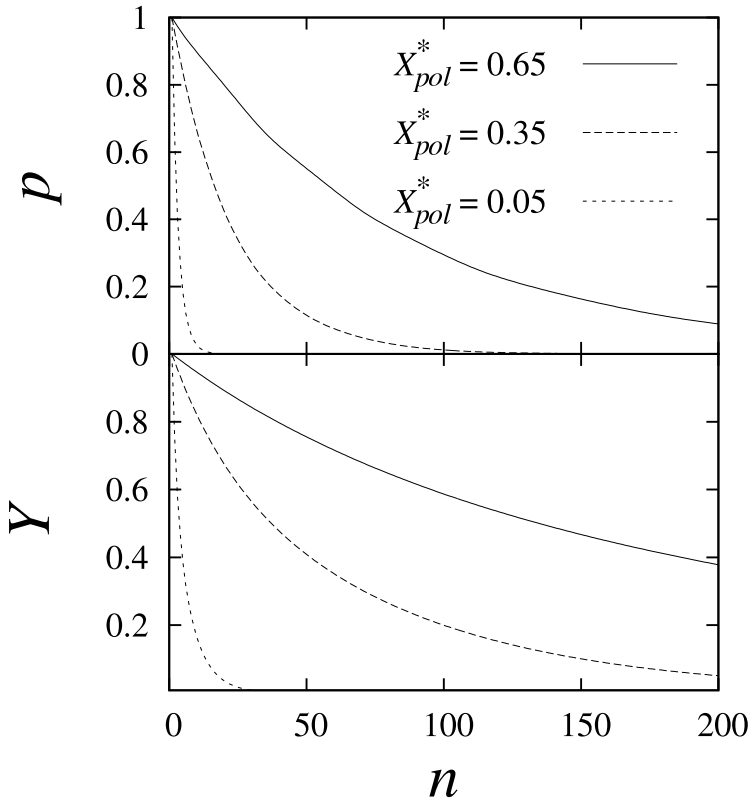

FIGURE 5.5. Plots of p and bifunctional monomer yield versus the number of purification steps. These plots were calculated directly from the phase diagram (Fig. 5.3).

In experimental systems, the fraction of chain stoppers is usually quite low even before purification. The relevant regime is therefore $p \to 0$, hence,

$$R_p = \frac{X^*_{pol}}{C_0\left(1-\alpha+\frac{\alpha X^*_{pol}}{C_0}\right)}, \tag{5.3}$$

$$R_Y = \frac{C_0\left(X^*_{pol}-D_0\right)}{X^*_{pol}\left(C_0-D_0\right)}. \tag{5.4}$$

Figure 5.6 shows that decay of p and Y is exponential, hence R_p and R_Y are constants that are given by Eqs. (5.3) and (5.4). The decay of p and Y with n is calculated by

$$p_n = p_0\left(R_p\right)^n, \tag{5.5}$$

$$Y_n = \left(R_Y\right)^n. \tag{5.6}$$

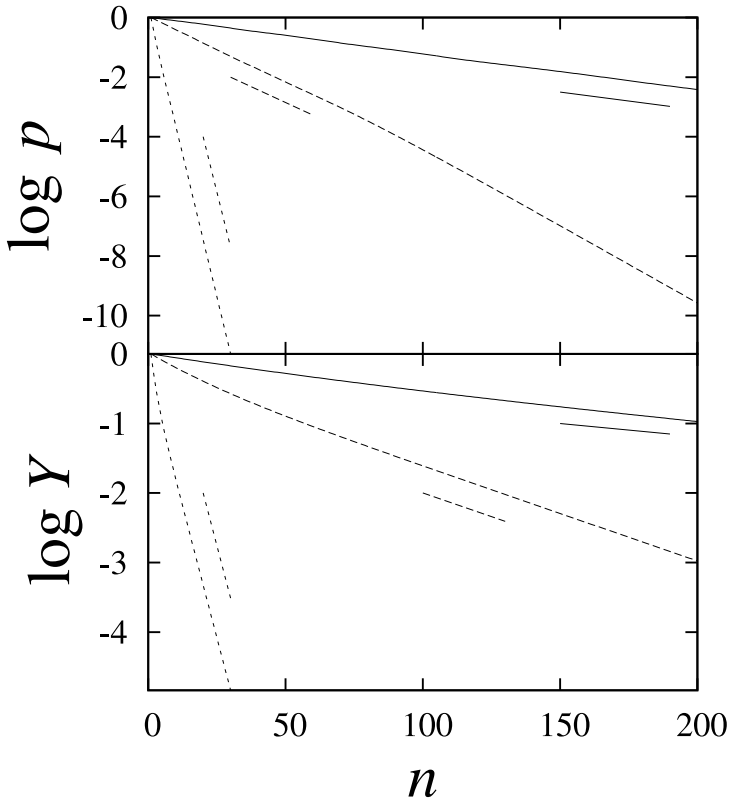

Figure 5.6. As in Fig. 5.5, but here the logarithms of p and Y are plotted against n. The short lines denote the slope of this plot calculated by Eqs. (5.3) and (5.4). Equations (5.3) and (5.4) give an accurate description the purification process, because the full plots and the short lines have the same slope.

It is hereby shown that α, C_0 and D_0 [by means of Eqs. (5.3) and (5.4)] are sufficient to describe the purification process. The parameters R_p and R_Y are central in describing the purification process because they determine the exponential decay rate of p and Y with the number of purification steps. The entire purification process can be calculated according to Eqs. (5.5) and (5.6). This leads to a great reduction in the computational demand of the calculation. Instead of calculating the entire phase diagram, only two simulations are needed to find C_0, D_0, and α: (i) one simulation without monofunctional monomers to find C_0 and D_0, and (ii) another simulation with monofunctional monomers to calculate α.

For a certain system at a certain temperature, the only process parameter that can be chosen is X^*_{pol}. Obviously, X^*_{pol} should be greater than D_0 but smaller than C_0.

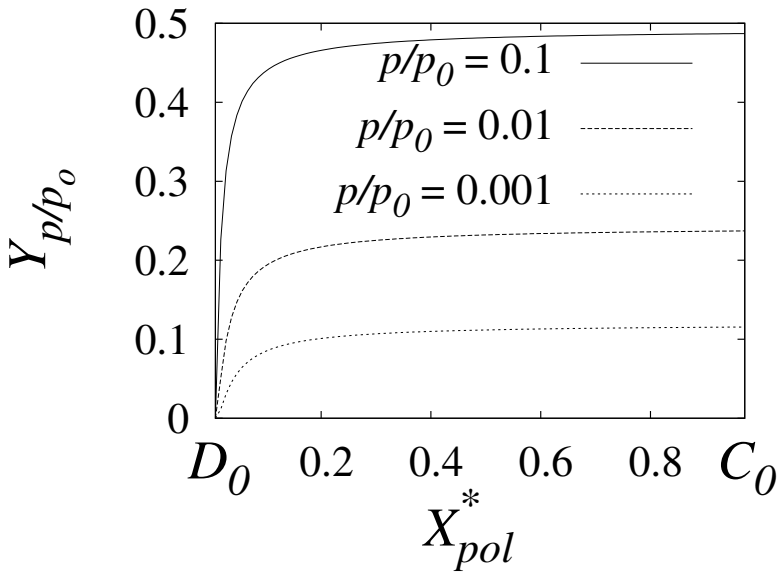

FIGURE 5.7. Plot shows the effect of the choice of X^*_{pol} on the yield when the purification parameter is reduced from p_0 to p. Equations (5.3), (5.4), (5.5), and (5.6) and the parameters from the phase diagram in Fig. 5.3 were used to construct this plot. Note that the highest possible yield is obtained when $X^*_{pol} \to C_0$. The maximum attainable yield can be calculated directly by means of Eq. (5.7).

We denote the number of purification steps that are needed to achieve a reduction of the purification parameter from p_0 to p as n_{p/p_0}. The yield after n_{p/p_0} steps is then Y_{p/p_0}. For practical purposes, it is interesting to calculate the effect of our choice of X^*_{pol} on n_{p/p_0} and Y_{p/p_0}. Obviously, n_{p/p_o} is equal to $\log(p/p_0)/\log R_p$ [Eq. (5.5)] and $Y_{p/p_0} = Y_0 \left(R_Y\right)^{n_{p/p_0}}$. The dependence of Y_{p/p_0} on X^*_{pol} is shown in Fig. 5.7. The yield vanishes when $X^*_{pol} \to D_0$ since $R_Y \to 0$ in that case [Eq. (5.4)]. The maximum yield can be obtained when X^*_{pol} is chosen to be very close to the composition of the concentrated phase:

$$\lim_{X^*_{pol} \to C_0} Y_{p/p_0} = \left(\frac{p}{p_0}\right)^{\frac{D_0}{(1-\alpha)(C_0-D_0)}} . \tag{5.7}$$

Therefore, the maximum yield that can be reached to reach a certain degree of purity is given by Eq. (5.7). Doing so would however require an infinite number of purification steps.

To fully exploit the possibilities of the phase diagram, we do not set X^*_{pol} to a fixed value for all values of E, but make X^*_{pol} depend on D_0 instead: $X^*_{pol} = \beta D_0$. We will use the parameter $\beta = X^*_{pol}/D_0$ to specify the choice of the polymer concentration. Obviously, $1 \leq \beta \leq C_0/D_0$. This leads to a very simple expression for R_Y in terms of

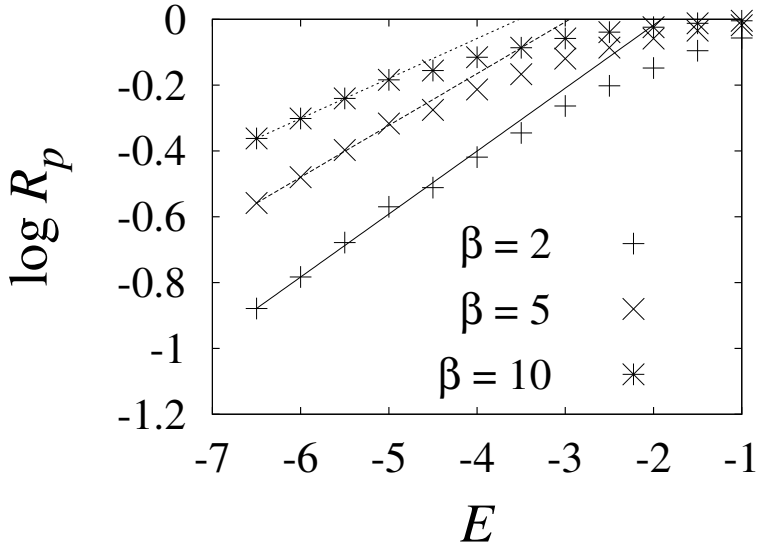

Figure 5.8. Values of R_p [calculated with Eq. (5.3)] are plotted logarithmically versus bond energy. Fits of R_p with emphasis on the low E regime are taken from Table 5.1 and shown by dashed lines. See text for computational details.

β [via Eq. (5.4)]:

$$R_Y \approx \frac{\beta - 1}{\beta}. \tag{5.8}$$

This is a very good approximation because $C_0 \approx 1 \gg D_0$, therefore, the approximation sign in Eq. (5.8) can be considered an equal sign for all practical purposes. Hence R_Y is found without any extrapolations necessary.

5.3.2. Predictions for realistic systems

It was shown that the phase diagram can be described by the three parameters C_0, D_0, and α for calculating the effectivity of purification. It is in principle possible to extrapolate all three parameters to realistic bond energies, and then calculate R_p and R_Y. However, estimating R_p and R_Y in this way is dangerous, because it depends on three different extrapolations. It is therefore preferable to extrapolate R_p directly, and calculate R_Y according to Eq. (5.8), for which no extrapolations are necessary.

To estimate R_p, we first calculated C_0, D_0, and α for a range of bond energies. The simulations were performed as described in Sec. 5.2, but with larger simulation boxes of $25 \times 25 \times 25$ lattice sites. We then calculated R_p by means of Eq. (5.3) and plotted R_p versus E (Fig. 5.8). Empirically fitted expressions for R_p are given in Table 5.1.

Because R_p and R_Y are now known, we can estimate the purification process at realistic bond energies. Figure 5.9 shows the dependence of n and Y on p/p_0 for $E = -20kT$. It can be inferred from Fig. 5.9 that we can expect to remove 99.9% of the chain stoppers ($p/p_0 = 10^{-3}$) and retain more than 50% of the bifunctional

Table 5.1. The calculated R_p values for different bond energies were fitted with emphasis on the regime of strong bonds to the empirical equation: $R_p = a10^{bE}$. The coefficients a and b are denoted in this table.

β	a	b
2	2.316	0.1913
5	2.911	0.1573
10	2.677	0.1215

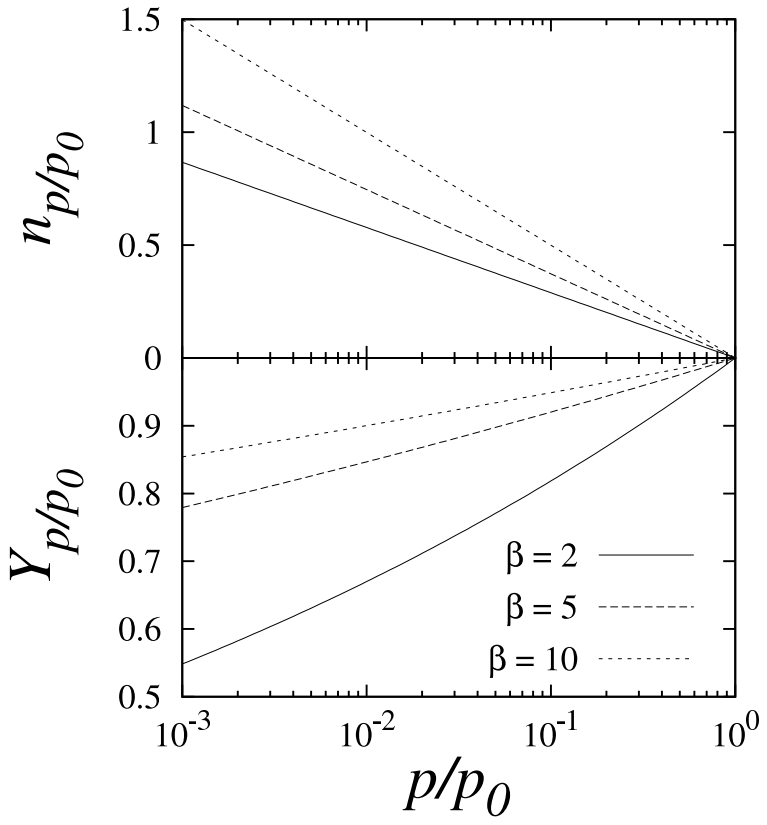

Figure 5.9. Predicted purification efficacy for $E = -20kT$. The value n_{p/p_0} is the number of purification steps that is needed to achieve a reduction of the purification parameter from p_0 to p. The yield after n_{p/p_0} steps is Y_{p/p_0}.

monomers after only one purification step if $\beta = 2$. If β is higher, that is, if less solvent is added in a single purification step, then a higher yield is possible. This would require only a few purification steps to reach the same level of purification.

It is clear that the volume of the concentrated phase will be much smaller than the volume of the dilute phase, even if $\beta = 10$. We recommend therefore that experimental conditions must be chosen so that the volume of the dilute phase is much greater than the volume of the concentrated phase. Which conditions should be chosen depends on the system and on the technical demands of the process. Once a suitable value of β is determined, one should determine D_0 by determining the concentration of supramolecular monomers in the dilute phase. With $X^*_{pol} = \beta D$ now known, there is enough information to set up the extraction process for this specific system.

5.4. Summary and outlook

In the previous sections, we have put forward a new method to remove monofunctional contaminants from supramolecular polymer solutions. The method exploits the partitioning of mono- and bifunctional monomers over the two phases of a phase-separated supramolecular polymer system. The polymer solution can be purified by discarding the dilute phase because that phase is enriched in monofunctional contaminants.

By means of a recently developed numerical technique, we calculated the entire phase diagram of a ternary mixture containing mono- and bifunctional monomers, and solvent. The purification process can be simulated directly from the phase diagram (Sec. 5.2).

Moreover, we were able to describe the purification process in terms of simple mathematical expressions with only three parameters. Only two simulations are necessary to find these parameters (Sec. 5.3.1). The effectivity of purification could therefore be calculated and extrapolated for a broad range of bond energies.

Our calculations indicate that one or two purification steps are sufficient to remove 99% of the chain stoppers while retaining about 80% of the bifunctional monomers in many experimental systems (Sec. 5.3.2). Higher yields are definitely possible if less solvent is added. However, some more purification steps are then required to reach the same purity of the sample.

The extraction method only involves the addition of solvent, so it is cheap to perform and could be easily scaled up to industrial quantities. It also does not require the addition of other chemicals that have to be removed afterward. In conclusion, the calculations presented in this chapter show that the present method is most likely a viable methodology to selectively and efficiently remove monofunctional ligands from supramolecular polymer solutions.

The next challenges are both computational and experimental. It would be of interest to assess the effect of solvency (which is not addressed in this chapter) and/or more complex molecular models on the effectivity and selectivity of purification. Finally, it is imperative to apply and test this method in experimental systems.

References

[1] L. Brunsveld, B. J. B. Folmer, E. W. Meijer, and R. P. Sijbesma, Chem. Rev. **101**, 4071 (2001).
[2] A. Ciferri, *Mechanisms of Supramolecular Polymerizations*, chapter 1, Supramolecular polymers (Ed. A. Ciferri), Marcel Dekker, New York, 2000.
[3] R. Sijbesma et al., Science **278**, 1601 (1997).
[4] P. S. Corbin and S. C. Zimmerman, *Hydrogen-Bonded Supramolecular Polymers*, chapter 4, Supramolecular polymers (Ed. A. Ciferri), Marcel Dekker, New York, 2000.
[5] E. A. Fogleman, W. C. Yount, Y. Xu, and S. L. Craig, Angew. Chem. Int. Ed. **41**, 4026 (2002).
[6] A. van de Craats et al., Adv. Mat. **11**, 1469 (1999).
[7] T. Vermonden et al., Macromolecules **36**, 7035 (2003).
[8] G. Armstrong and M. Buggy, J. Mat. Sci. **40**, 547 (2005).
[9] M. E. Cates and S. J. Candau, J. Phys.: Condens. Matter **2**, 6869 (1990).
[10] J. des Cloizeaux and G. Jannink, *Polymers in Solution*, Clarendon Press, Oxford, 1990.
[11] D. Frenkel and B. Smit, *Understanding Molecular Simulation*, Academic Press, London, 2002.
[12] A. Milchev and D. P. Landau, J. Chem. Phys. **104**, 9161 (1996).
[13] Y. Rouault and A. Milchev, Macromol. Theory Simul. **6**, 1177 (1997).
[14] J. P. Wittmer, A. Milchev, and M. E. Cates, J. Chem. Phys. **109**, 834 (1998).
[15] A. Milchev, J. P. Wittmer, P. van der Schoot, and D. P. Landau, Europhys. Lett. **54**, 58 (2001).
[16] X. Lü and J. T. Kindt, J. Chem. Phys. **120**, 10328 (2004).
[17] A. Z. Panagiotopoulos, Mol. Phys. **61**, 813 (1987).
[18] H. J. A. Zweistra and N. A. M. Besseling, Phys. Rev. E **74**, 016111 (2006).
[19] W. L. Jorgensen and J. Pranata, J. Am. Chem. Soc. **112**, 2008 (1990).
[20] J. Pranata, S. G. Wierschke, and W. L. Jorgensen, J. Am. Chem. Soc. **113**, 2810 (1991).

Summary

This thesis describes theoretical results of supramolecular polymers in inhomogeneous systems. Supramolecular polymers are linear assemblies of which the monomers are joined by reversible bonds. Many types of supramolecular polymers have been synthesized in recent years. Moreover, there are numerous compounds in nature which exhibit similar behavior. Simulations of coarse-grained models of supramolecular polymers yielded new insights into the properties of supramolecular polymers in inhomogeneous systems.

Self-consistent-field calculations on the quasi-chemical level of approximation were used to obtain information about adsorbed supramolecular polymers (chapters 2 and 3). In chapter 2, we describe the effect of adsorption on the mean chain length of supramolecular polymers. It is generally agreed that $\langle N \rangle$ always increases with concentration in homogeneous systems. Adsorbed supramolecular polymers exhibit qualitatively different if the adsorption energy per segment is strong enough. A very interesting non-monotonical concentration dependence of $\langle N \rangle$ of adsorbed supramolecular polymers was found. In other words: there exists a regime where $\langle N \rangle$ *decreases* with increasing concentration. This has never been shown before. The physical background is a change of the structure of the adsorbed layer: the adsorbed layer changes from flat to fluffy when the monomer concentration is increased.

Chapter 3 also deals with adsorbing supramolecular polymers, but focuses on the adsorbed amount. This chapter describes how the model parameters influence the shape and position of the adsorption isotherms. Moreover a comparison is made with the adsorption isotherms of macromolecular polymers. It is found that supramolecular polymers adsorb at relatively high volume fractions and the filling of the surface occurs within a narrow range of concentrations. As a result, supramolecular polymers can be desorbed from the surface by diluting the surrounding solution. Macromolecular polymers usually cannot be desorbed in this manner. This has important implications for the use of supramolecular polymers as surface-active agents since the usefulness increases when they can be removed from the surface. Cleaning the surface requires little effort: diluting the surrounding solution is sufficient.

Chapters 4 and 5 describe a different type of inhomogenous systems: phase-separated systems. The results of these chapters were obtained by Monte Carlo simulations. In chapter 4, we introduce the "Helmholtz ensemble", a formalism to calculate the compositions of two coexisting liquid phases by a Monte Carlo simulation. The general

idea of this method is to use three simulation boxes (or more, if more than two coexisting phases are present). The only perturbations that are needed are molecule swaps and changes in the orientation of the molecules. Molecule displacements are only needed if a continuum model is used. Unlike the well-known Gibbs ensemble method, volume moves are unnecessary. As a consequence, an interface is formed in one of the simulation boxes. The compositions of the simulation boxes that contain homogeneous phases are used to obtain the compositions of the coexisting liquids.

For a succesful simulation it is required that a flat interface is formed. Several tests are proposed to check the net curvature of the interface. If a curved interface is formed, then the simulation should be repeated with a different starting composition. The restraint that a flat interface should be formed therefore does not affect the range of applicability of the technique. The Helmholtz ensemble method is especially useful for liquids that are modeled on a lattice, since no volume moves are necessary as is the case in the (related) Gibbs ensemble method. It is shown that the Helmholtz ensemble reproduces the phase behavior of the 3D Ising problem very accurately.

Supramolecular polymer systems are often polluted by monofunctional contaminants which are very difficult to remove. A new purification method aimed specifically at removing monofunctional contaminants is put forward in chapter 5. The idea is to decrease the solvent quality (e.g., by cooling) and to let the supramolecular polymer solution separate into two phases. It is to be expected that the phase that is poor in polymer has a relatively high concentration of monofunctional monomers. Therefore the solution can be purified by discarding the dilute phase.

In chapter 5, the effectivity of the proposed purification method is investigated by means of Monte Carlo simulations. The compositions of the concentrated and the dilute coexisting phases are calculated by means of the Helmholtz ensemble method. The entire phase diagram of bifunctional monomers, monofunctional molecules and solvent can be constructed. The efficiency of the several purification steps could be calculated directly from the phase diagram. Moreover, a parameterization of the phase diagram can be found. For purification purposes, the phase diagram can be described by three parameters. Only two simulations are needed to obtain these parameters. It therefore becomes feasible to predict the effectivity of the purification method for a wide range of linking energies. Extrapolations show that the vast majority of monofunctional contaminants can be removed by a single purification step if the conditions are well chosen. Several recommendations for experimental systems are also provided.

Samenvatting voor niet-vakgenoten

Deze samenvatting is bedoeld voor niet-vakgenoten die graag willen begrijpen waar dit proefschrift over gaat. Eerst zal de titel verklaard worden waardoor het onderwerp van dit proefschrift duidelijk wordt. Daarna zullen de belangrijkste resultaten de revue passeren.

Onderwerp van dit proefschrift

De vertaling van de titel van dit proefschrift luidt in gewoon Nederlands: "Supramoleculaire polymeren in inhomogene systemen". Omdat mogelijk niet alle termen in de titel duidelijk zijn, worden alle termen afzonderlijk uitgelegd.

Het begrip **systeem** heeft in de natuurwetenschappen een specifieke betekenis. Een systeem is datgene dat onderzocht wordt. Er bestaan vele soorten systemen. We kunnen hierbij onderscheid maken tussen *homogene* en **inhomogene** systemen. Bij homogene systemen maakt het niet uit welk gedeelte van het systeem onderzocht wordt; de eigenschappen zijn overal hetzelfde. Alhoewel alleen vacuüm ècht homogeen is, wordt deze term meestal iets losser gehanteerd. Systemen zijn dan homogeen als ze uit één fase bestaan. Denk bijvoorbeeld aan een cylinder met gas of een zoutoplossing. Inhomogene systemen bestaan uit meerdere fasen. Denk bijvoorbeeld aan een glas water met een ijsklontje erin: dit systeem bestaat uit twee fasen en is daarom inhomogeen. Een tweede voorbeeld van een inhomogeen systeem is verf. De pigmenten die verf zijn kleur geven zijn meestal onoplosbare poeders. Verf bestaat dus uit een vaste fase (pigment) en een vloeistoffase (oplosmiddel, zie ook figuur 1). Het is vaak zo dat inhomogene systemen uit een vaste en een vloeibare fase bestaan, maar dit hoeft niet het geval te zijn. Een systeem met twee slecht-mengbare vloeistoffen (bijvoorbeeld olie en water) zal spontaan in twee fasen uiteenvallen, en is daarmee een inhomogeen systeem met twee *coëxisterende* vloeistoffasen geworden. Een kenmerk van inhomogene systemen is dat er *grensvlakken* bestaan tussen de verschillende fasen. In het systeem met het smeltende blokje ijs bestaat er een grensvlak tussen het ijs en het vloeibare water. In verf bevinden zich vele grensvlakken tussen de pigmentdeeltjes en het oplosmiddel.

Polymeren zijn moleculen die lang en dun van vorm zijn. Ze zijn ongebouwd uit *segmenten* die met elkaar verbonden zijn. In de natuur komen polymeren op zeer veel plaatsen voor. Bekende voorbeelden zijn: cellulose, glycogeen en zetmeel. De segmenten van deze polymeren zijn glucose moleculen. Door de segmenten aan elkaar te verbinden, ontstaat een heel groot molecuul. Omdat het polymeer uit één heel groot

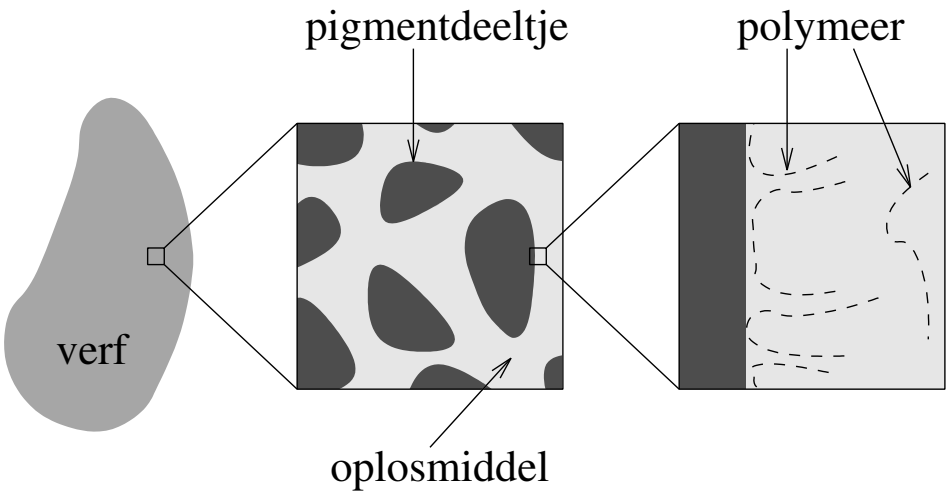

FIGUUR 1. Links is een klodder verf te zien waarop steeds verder ingezoomd wordt. Verf is een inhomogeen systeem en bestaat uit meerdere fasen: in dit geval vaste pigmentdeeltjes en vloeibaar oplosmiddel. De in het oplosmiddel aanwezige polymeren zijn ook afgebeeld. Deze polymeren kunnen adsorberen aan het grensvlak tussen pigmentdeeltje en oplosmiddel, en veranderen daarmee de eigenschappen van dat grensvlak.

molecuul bestaat, wordt zoiets een *macromolecuul* genoemd. Overigens, polymeren zijn ook van enorme industriële betekenis: plastic, rubber, nylon (en nog veel meer materialen) bestaan bijna uitsluitend uit polymeren.

Een systeem met polymeren wordt vaak vergeleken met een bord spaghetti. Dit is niet zo'n hele goede vergelijking omdat polymeren bij kamertemperatuur continu in beweging zijn. Een bak met wriemelende wormen is wellicht een betere metafoor. Door de langgerekte vorm hebben polymeren enkele heel interessante en unieke eigenschappen. Typerend gedrag van polymere systemen is elastisticiteit, dat is het vermogen van een materiaal om na vervorming weer de oorspronkelijke vorm aan te nemen. Elastiek heeft niet voor niets die naam gekregen, en elastiek is dan ook gemaakt van polymeren.

Een belangrijk toepassingsgebied van polymeren is modificatie van grensvlakken. Polymeren worden op deze manier toegepast in o.a. verf, fotografisch filmmateriaal en protheses. Veel polymeren kunnen "plakken" aan grensvlakken, een proces dat *adsorptie* genoemd wordt (figuur 1). De eigenschappen van het grensvlak veranderen meestal ingrijpend als er polymeren op dat grensvlak adsorberen. Vaak zullen de polymeren ervoor zorgen dat de grensvlakken elkaar zullen afstoten. Dit kan handig zijn: pigmentdeeltjes zullen minder snel samenklonteren als er polymeren op geadsorbeerd zijn. Maar afhankelijk van de omstandigheden kan het ook zijn dat toevoeging van polymeren juist de samenklontering bevordert. Gedetailleerde kennis is vaak nodig om het precieze effect van het toevoegen van polymeren te kunnen voorspellen.

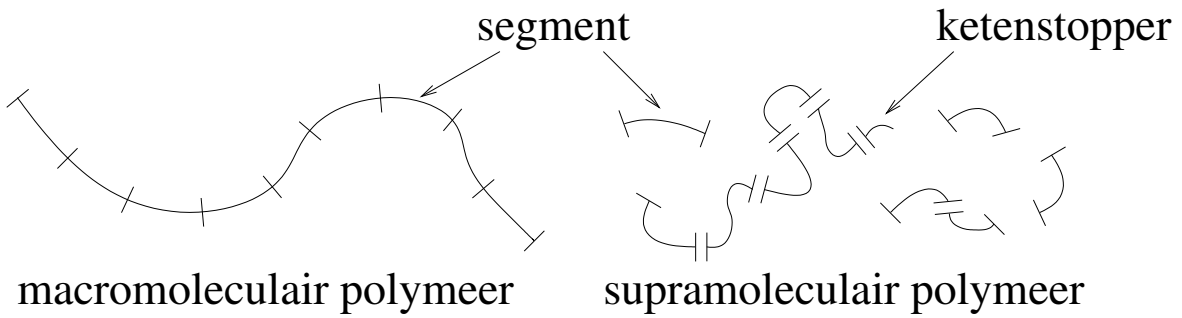

Figuur 2. Deze figuur laat het verschil zien tussen gewone macromoleculaire polymeren en supramoleculaire polymeren. De segmenten van macromoleculaire polymeren zijn stevig aan elkaar verbonden. De lengte van het polymeer ligt dus vast op het moment dat het geproduceerd wordt. Supramoleculaire polymeren zijn opgebouwd uit segmenten die losjes aan elkaar zitten. De lengte van dit type polymeer hangt af van de omstandigheden in het systeem, zoals temperatuur en segmentconcentratie. De segmenten van de supramoleculaire polymeren bestaan meestal uit twee "plakkers" die met een tussenstuk zijn verbonden. Misvormde segmenten die maar één plakker bezitten, worden wel *ketenstoppers* genoemd, omdat de keten niet verder kan groeien als er een ketenstopper aan bindt.

De meest kenmerkende eigenschap van een polymeermolecuul is zijn lengte. Het is gebleken dat veel eigenschappen van polymeren alleen afhangen van de lengte en niet van de eigenschappen van de segmenten. De lengte van een macromolecuul kan niet zomaar veranderd worden. Voor bepaalde toepassingen kan het handig zijn om over polymeren te beschikken waarvan de lengte wel veranderd kan worden. Men heeft dit bereikt door segmenten te ontwikkelen die reversibel aan elkaar binden. De segmenten van zo'n molecuul zijn ieder afzonderlijke moleculen. Een polymeer dat opgebouwd is uit zulke segmenten bestaat uit een serie moleculen en wordt daarom een **supramoleculair** polymeer genoemd.

In tegenstelling tot een macromolecuul zijn de bindingen van een supramoleculair polymeer reversibel. De reden hiervoor is dat de kracht die een molecuul bij elkaar houdt vele malen sterker is dan de kracht waarmee afzondelijke moleculen aan elkaar blijven plakken. In figuur 2 worden de verschillen tussen macromoleculaire en supramoleculaire polymeren uitgelegd.

De lengte van een supramoleculair polymeer varieert continu vanwege de reversibele bindingen. In een systeem met supramoleculaire polymeren zijn altijd vele verschillende polymeerlengtes aanwezig. Deze systemen worden daarom meestal gekarakteriseerd door de *gemiddelde ketenlengte*. Het is gebleken dat de gemiddelde ketenlengte gestuurd kan worden zonder de chemische identiteit van de polymeren te veranderen. Er wordt heel wat verwacht van dit nieuwe type polymeer en er worden veel toepassingen voorzien,

vooral in de nanotechnologische hoek. De laatste jaren is er al veel onderzoek op dit terrein verricht, zowel experimenteel als theoretisch. Dit proefschrift is een theoretische verhandeling die bepaalde aspecten van supramoleculaire polymeren in inhomogene systemen beschrijft.

Belangrijkste resultaten

Met behulp van computersimulaties werden twee typen inhomogene systemen bestudeerd: systemen met een vast-vloeistof grensvlak en systemen die bestaan uit twee coëxisterende vloeistoffasen. Aan deze twee typen systemen zijn ieder twee hoofdstukken gewijd. Als in dit gedeelte "concentratie" genoemd wordt, wordt hiermee de segmentconcentratie bedoeld.

In **hoofdstuk 2** wordt de gemiddelde ketenlengte van geadsorbeerde en ongeadsorbeerde supramoleculaire polymeren met elkaar vergeleken. Het verschil bleek in veel gevallen groot te zijn. De gemiddelde ketenlengte van ongeadsorbeerde supramoleculaire polymeren neemt altijd toe met concentratie. Voor flexibele geadsorbeerde polymeren is dit niet per definitie zo: als de adsorptiekracht groot genoeg is, dan kan het zijn dat de gemiddelde ketenlengte *afneemt* met concentratie. Dit is dus het tegenovergestelde van wat er voor ongeadsorbeerde polymeren werd gevonden. Een verklaring voor dit verschil wordt ook beschreven in dit hoofdstuk.

Hoofdstuk 3 gaat net als het vorige hoofdstuk over geadsorbeerde supramoleculaire polymeren. In dit hoofdstuk staat de geadsorbeerde hoeveelheid segmenten als functie van de concentratie centraal. Het bleek dat supramoleculaire polymeren van het grensvlak verwijderd kunnen worden als de concentratie maar laag genoeg gemaakt wordt. Voor macromoleculen is dit praktisch ondoenlijk. In dit hoofdstuk wordt verder in vrij groot detail de oorzaken van dit verschil in gedrag besproken.

Systemen met supramoleculaire polymeren zijn vaak vervuild met "ketenstoppers" (figuur 2). Deze ketenstoppers zijn schadelijk want ze verstoren de ketenvormingscapaciteit van de supramoleculaire polymeren. In **Hoofdstuk 5** wordt een voorstel gedaan voor een methode om deze ketenstoppers te verwijderen. Met simulaties is onderzocht hoe efficiënt deze methode zou kunnen zijn. De methode is eenvoudig: de mengbaarheid van het oplosmiddel en de supramoleculaire polymeren moet verlaagd worden (door b.v. de temperatuur te verlagen). Hierdoor ontstaan twee coëxisterende vloeistoffasen: een fase met voornamelijk oplosmiddel en een fase met voornamelijk polymeer. In de oplosmiddelfase zullen relatief veel ketenstoppers voorkomen. Het systeem kan gezuiverd worden door de oplosmiddelfase weg te gooien en de polymeerfase te behouden. Met bestaande simulatiemethoden bleek het zeer moeilijk en tijdrovend te zijn om dit te onderzoeken. Er is daarom een nieuwe simulatietechniek ontwikkeld die beschreven staat in **hoofdstuk 4**. Deze simulatietechniek is gedoopt tot "Helmholtz-ensemble methode". De methode is ook bruikbaar buiten de context van supramoleculaire polymeren.

List of publications

H. J. A. Zweistra, C. C. M. Samson, and W. Klopper, *Similarity-transformed Hamiltonians by means of Gaussian-damped interelectronic distances*, Collection of Czechoslovak Chemical Communications **68(2)**, 374-386, (2003). (graduate work)

H. J. A. Zweistra and N. A. M. Besseling, *Mean chain length of adsorbed supramolecular polymers*, Physical Review Letters **96(7)**, 078301, (2006). (chapter 2)

H. J. A. Zweistra and N. A. M. Besseling, *Direct determination of liquid phase coexistence by Monte Carlo simulations*, Physical Review E **74**, 016111, (2006). (chapter 4)

H. J. A. Zweistra, N. A. M. Besseling, and M. A. Cohen Stuart, *Monte Carlo study of supramolecular polymer fractionation: Selective removal of chain stoppers by phase separation*, Journal of Physical Chemistry B **110(37)**, 18629-18634, (2006). (chapter 5)

H. J. A. Zweistra and N. A. M. Besseling, *Adsorption and desorption of reversible supramolecular polymers*, Physical Review E **74**, 021806, (2006). (chapter 3)

Dankwoord

Het moge duidelijk zijn: het boekje is af. Het is dus tijd om terug te kijken op de periode waarin dit werkstukje tot stand kwam. Ik denk met plezier terug aan de afgelopen jaren en er is een aantal mensen dat ik hiervoor zou willen bedanken, wat ik dus bij deze doe.

Ik heb gemerkt dat het schrijven van een proefschrift geen solitaire bezigheid is. Bij deze bedank ik alle studenten, stafleden, post-doc's en promovendi op Fysko voor de uitermate goede werksfeer waarin er altijd ruimte was voor creativiteit en gezelligheid. Er zijn een aantal mensen die in het bijzonder iets hebben bijgedragen aan de totstandkoming van dit boekje.

Klaas, ik heb veel van je geleerd en jij hebt zonder twijfel een grote invloed gehad op de inhoud van dit proefschrift. Onze manier van samenwerken, en vooral ons wederzijdse open-deur beleid, heb ik altijd als zeer prettig ervaren.

Gerard, jij raakte pas in een relatief laat stadium direct betrokken bij de inhoud van dit boekje. Toch heeft jouw invloed zeker geholpen bij het proces van het afleveren van het proefschrift. Inhoudelijk gezien was jouw inbreng in met name hoofdstuk 3 zeer waardevol.

Vele discussies met fysko-ers hebben hun weerslag gevonden in het proefschrift. De personen voor wie dit in sterke mate geldt, wil ik nog in het bijzonder benoemen. Martien, jij was dan niet mijn promotor maar toch altijd verbazend goed op de hoogte wat ik uitspookte. Jouw suggesties waren vaak erg nuttig: als jij niet met het idee gekomen was om ketenstoppers met extractie te verwijderen, waren hoofdstukken 4 en 5 er niet in deze vorm geweest. Frans, ik herinner me nog goed het vak Moleculaire Thermodynamica dat ik jaren geleden bij jou gevolgd heb. Er waren toen tamelijk weinig studenten voor dat vak, maar jouw privécolleges hebben destijds wel mijn interesse voor dit vakgebied gewekt. Renko, bedankt voor je inbreng over het Helmholtz ensemble, dit heeft sterk bijgedragen aan hoofdstuk 4. Jasper, ik heb uiteraard veel gebruik gemaakt van jouw voorbereidend werk op dit vakgebied, bedankt daarvoor.

Ronald, ik zou jou graag willen bedanken voor de ondersteuning voor alles wat standaard en niet-standaard is. Peter, bedankt voor je hulp toen ik mijn eerste schreden op het C++-pad maakte. Verder zou ik je willen bedanken voor het onderhoud van de rekencomputers. Remco, helaas bleek de installatie om adiabatische en reversibele gascompressie te demonstreren niet te werken. De theorie was kennelijk mooier dan de praktijk.

Yansen, je was echt een fijne kamergenoot met wie het goed converseren was over wetenschappelijke en minder wetenschappelijke onderwerpen. Veel succes met je post-doc in Edmonton.

De Student Conference was zonder enige twijfel een hoogtepunt van mijn promotietijd. Wout, Maykel en Bart: bedankt voor de prettige en harmonieuze samenwerking. Ik denk ook met veel genoegen terug aan het copieuze diner in restaurant "Het Koetshuis".

Tenslotte wil ik nog noemen: Renate, Olga, Maarten, Wouter, Richard en Diane.

Robert en Marco, leuk dat jullie mijn paranimfen willen zijn.

Ma, dank je wel voor het vertrouwen in mij. Pa, dank je wel voor je enthousiasme en levenswijsheden. Ik zal me niet laten verrassen.

Maris, er zijn heel veel leuke en een paar minder leuke dingen gebeurd sinds ik aan het promotieonderzoek begon. Na jaren van uitgebreid onderzoek en heel wat formules hebben we nu allebei een proefschrift. Je bent mijn spiegel en belangrijkste inspiratiebron en ik wil je ontzettend bedanken dat je er altijd geweest bent en hopelijk nog heel lang zult zijn.


Henk

Levensloop

Henk Zweistra werd op 25 juli 1978 geboren te Den Haag, alwaar hij in 1996 zijn VWO-diploma behaalde. In datzelfde jaar startte hij de studie Bioprocestechnologie in Wageningen. Rond de millenniumwisseling besloot hij een vrij doctoraal programma te volgen waardoor het zwaartepunt van de studie op de theoretische chemie kwam te liggen. De bul werd in januari 2003 uitgereikt. De studie omvatte een hoofdvak Theoretische Chemie (Universiteit Utrecht) en een afstudeervak Moleculaire Fysica (Wageningen Universiteit). Tevens heeft hij in 2002 stage gelopen bij professor Doi aan het Department of Computational Science and Engineering in Nagoya, Japan. In december 2002 startte hij een promotieonderzoek aan het Laboratorium voor Fysische Chemie en Kolloïdkunde in Wageningen met als belangrijkste resultaat het boekje dat u nu in handen heeft. Op 1 juli 2006 trad hij in dienst bij ABN AMRO op de afdeling Risk Management.

Overview of completed training activities

Name of the course	Location/Institute	Year
Discipline specific activities		
Polymer physics course	PTN	2003
Winterschool "Dynamics"	Han-sur-Lesse, Belgium	2003
Winterschool "Statics"	Han-sur-Lesse, Belgium	2004
Conference "Statistical Physics"	Veldhoven	2004
ECIS conference	Almería, Spain	2004
Advanced colloid course	Universiteit Utrecht	2005
Student conference	Biezenmortel	2005
Conference "Macromolecules"	Lunteren	2005
Conference "Macromolecules"	Lunteren	2006
General courses		
Presentation skills	FOM	2004
Planning	FOM	2005
Business orientation program	Universiteit Nyenrode	2006
Optionals		
Work group meeting	WUR	2002-2006
Colloquia	WUR	2002-2006
Preparation PhD research proposal		